TARGETING MIRNA-PROTEIN REGULATORY NETWORKS TO ENHANCE CHEMOTHERAPY RESPONSE IN *BRCA1*-MUTATED TNBCs

A THESIS SUBMITTED TO
THE GRADUATE SCHOOL OF ENGINEERING AND SCIENCE
OF BILKENT UNIVERSITY
IN PARTIAL FULFILLMENT OF THE REQUIREMENTS FOR
THE DEGREE OF
MASTER OF SCIENCE
IN
MOLECULAR BIOLOGY AND GENETICS

By

Erol Eyüpoğlu

August 2016

TARGETING MIRNA-PROTEIN REGULATORY NETWORKS TO ENHANCE CHEMOTHERAPY RESPONSE IN *BRCA1*-MUTATED TNBCs

By Erol Eyüpoğlu

August, 2016

We certify that we have read this dissertation and that in our opinion it is fully adequate in scope and in quality, as a thesis for the degree of Master of Science.

_____

Özgür Şahin

(Advisor)

_____

Serkan İsmail Göktuna

_____

A. Elif Erson Bensan

Approved for Graduate School of Engineering and Science

_____

Levent Onural

Director of the Graduate School of Engineering and Science

ABSTRACT

TARGETING MIRNA-PROTEIN REGULATORY NETWORKS TO ENHANCE CHEMOTHERAPY RESPONSE IN *BRCA1*-MUTATED TNBCs

Erol Eyüpoğlu

M.S. in Molecular Biology and Genetics

Advisor: Özgür Şahin

August, 2016

Breast cancer is the second most common cancer and the leading cause of cancer associated deaths in women worldwide. Triple-negative breast cancer (TNBC) is the most aggressive subtype of breast cancer. *BRCA1*-mutated TNBC patients generally respond well to DNA cross-linking agents like Cisplatin. However, most of the patients acquire resistance and eventually die. Therefore, there is a dire need of developing promising approaches to enhance chemo-response, hence, extending the survival of TNBC patients. MicroRNAs (miRNAs) play active role in controlling proliferation, apoptosis, invasion and drug resistance in cancer. However, the role of miRNA-protein interactions as a regulatory network in determining chemotherapy response of TNBCs has not been elucidated yet. Thus, we aimed to delineate miRNAs and miRNA-protein regulatory networks controlling chemotherapy resistance/response in *BRCA1*–mutated TNBCs. We firstly confirmed that BRCA1-mutated breast cancer cells are more sensitive to Cisplatin as compared to BRCA1-competent cells. Afterwards, developing acquired chemotherapy resistant cell line model and using next generation sequencing technology (both miR-Seq and RNA-Seq), we have unravelled that p53 signalling is the upstream regulator of Cisplatin resistance. Moreover, with the use of Ingenuity Pathway Anlaysis (IPA) which uses omics data from a variety of experimental platforms, we analyzed, combined and modelled miRNA-mRNA interactions regulating Cisplatin resistance for the first time in a network

manner. Interestingly, we identifed several network motifs e.g. coherent and incoherent feedforward loops centered around p53 protein which need further experimental validations. Again for the first time, this study has reported the re-sensitization effect of miR-455 family on Cisplatin resistance in breast cancer. Overall, findings of this study might be used as an alternative strategy for treatment of *BRCA1*-mutated TNBCs by modulating miRNAs and their targets to re-sensitize Cisplatin resistant tumors.

Keywords: Triple-negative breast cancer, chemotherapy resistance, microRNAs, microRNA-protein regulatory networks, systems biology, *BRCA1*, miR-455, p53 signalling.

ÖZET

BRCA1 MUTASYONU OLAN TRİPLE-NEGATİF MEME KANSERİNDE KEMOTERAPİ YANITINI ARTTIRMAK İÇİN MİKRORNA-PROTEİN ETKİLEŞİM AĞLARININ HEDEFLENMESİ

Erol Eyüpoğlu

Moleküler Biyoloji ve Genetik, Yüksek Lisans

Tez Danışmanı: Özgür Şahin

Ağustos, 2016

Meme kanseri dünya çapında en sıklıkla görülmekte olan 2. kanser türü ve kadınlarda kanser kaynaklı ölümlerin ilk sırasında yer almaktadır. Triple-negatif meme kanseri (TNMK) meme kanseri alt-grupları arasındaki en agresif türdür. *BRCA1* geni mutasyonlu TNMK hastaları Cisplatin gibi DNA çapraz bağlayıcı ilaçlarına başlangıçta iyi cevap verselerde, hastaların çoğunda zamanla direnç gelişir ve direnç kaynaklı ölüm görülür. Bu nedenle, bu hastalarda kemotrapi cevabını iyileştirerek hastaların sağkalımını arttırmak elzemdir. mikroRNAlar (miRNAs), kanserde; proliferasyon, apoptoz, invazyon ve ilaç direncinin düzenlenmesinde aktif rol alırlar. Ancak, TNMK'de, mikroRNA-protein etkileşimlerinin bir ağ şeklinde düzenlenerek kemoterapi cevabındaki rolü bugüne kadar gösterilmemiştir. Bu nedenle, bu tezde, BRCA1 geni mutasyonlu hastaların kemoterapi direnç/hassasiyetini kontrol eden miRNAlar ve miRNA-protein etkileşim ağlarının bulunması hedeflenmiştir. Çalışmalarımıza BRCA1 geni mutasyonlu TNMK hücre hatlarının olmayanlara göre Cisplatine daha sensitif olduğunu göstererek başladık. Sonrasında, sonradan kazanılan Cisplatine dirençli hücre hattı modeli geliştirip, bu hücre hatlarını yeni nesil dizileme yöntemleri (miR-Seq ve RNA-Seq) ile sekanslatarak, p53 sinyal yolağının Cisplatin direncini düzenlediğini gösterdik. Buna ek olarak, birçok deneysel kaynaktan elde edilen omik verileri kullanan Ingenuity Yolak Analizi (IYA)

programını kullanarak, Cisplatin direncinde rol oynayan miRNA-mRNA etkileşimlerini ilk kez bir ağ şeklinde göstermiş bulunmaktayız. İlginç bir şekilde, p53 proteini etrafında merkezi bir öneme sahip ağ motiflerinin varlığını tespit ettik. Meme kanserinde miR-455 ailesinin Cisplatin dirençli hücrelerde ilaca hassasiyet sağladığını da ilk kez gösterdik. Sonuç olarak, bu çalışma *BRCA1* geni mutasyonlu hastalarda, miRNAlar ve hedeflerinin düzenlenerek, ilaca karşı tekrar hassasiyet sağlandığı bir tedavi seçeneği olma potansiyeli taşımaktadır.

Anahtar Kelimeler: Triple-negatif meme kanseri, kemoterapi direnci, microRNAlar, microRNA-protein düzenleyici ağları, sistem biyolojisi, *BRCA1*, miR-455, p53 sinyali.

Acknowledgements

I would like to say a sincere thank you to Dr. Özgür Şahin for giving me this great opportunity and directing me with his wise academic experience in my master's study.

I would like to acknowledge Umar Raza for his life-saving efforts with Western Blot experiments and his priceless support and friendship in every stage of this work. I also would like to thank Özge Saatci and Pelin Ersan for their valuable help in qPCR experiments.

I would like to thank all members of Şahin Lab: Merve Mutlu, Emre Yurdusev, Hilal Bal, Ünal Metin Tokat, Özge Akbulut, Selvi Durmuş, Suhail Ansari, and Rashmi Mishra for their help and support.

I express a deep sense of gratitude to the Scientific and Technological Research Council of Turkey (TÜBİTAK), European Molecular Biology Organization (EMBO) and the Turkish Academy of Sciences (TÜBA) for their financial support to do this thesis.

I would like to thank Ali Can Savaş for his great friendship and help.

Finally, I would like to thank Özge Başer for her support in all aspects of my life.

This thesis is funded by TUBITAK Project Number: 114C060.

Teşekkür

Derin akademik bilgisi ve tecrübeleriyle, beni bu süreçte yönlendiren ve her konuda desteğini esirgemeyen ve dolayısıyla bu çalışmadaki ‘Aslan Payı’ nın sahibi Yrd. Doç. Dr. Özgür Şahin’e,

Bu çalışmanın her evresindeki paha biçilemez desteği ve arkadaşlığının yanı sıra, Western Blot deneylerindeki hayat kurtarıcı yardımı sebebiyle Umar Raza’ya,

Hiçbir konuda sizi geri çevirmeyen, her zaman yapabileceği yardımın en iyisini sunan Özge Saatci’ye qPCR deneylerindeki desteği ve ona uykusundan feragat ederek yardımcı olan Pelin Ersan’a,

Ekip ruhunu yakaladığımız tüm Özgür Şahin Lab üyelerine: Merve Mutlu, Emre Yurdusev, Hilal Bal, Ünal Metin Tokat, Özge Akbulut, Selvi Durmuş, Suhail Ansari, and Rashmi Mishra’ya,

Bu tezin bitirilebilmesi için finansal destek sağlayan TÜBİTAK, EMBO ve TÜBA’ya,

Her zaman yardımıma koşup, en içten desteğini sunan dostum Ali Can Savaş’a (nam-ı diğer Caniko),

Ve son olarak, her zaman olduğu gibi bu zorlu süreçte de sevgisini hissettiğim, beni destekleyerek yalnız bırakmayıp uzakları yakın eden Özge Başer’e,

Sonsuz teşekkür ve şükranlarımı sunarım.

Bu tez TÜBİTAK 114C060 numaralı proje bütçesi ile gerçekleştirilmiştir.

Table of Contents

List of Figures

List of Tables

Abbreviations

APS	Ammonium peroxodisulfate
BCA	Bicinchoninic acid
BRCA1	Breast cancer type 1 susceptibility protein
BSA	Bovine Serum Albumin
CDH1	E-cadherin
CDK2	Cyclin-dependent kinase 2
DMEM	Dulbecco's Modified Eagle Medium
DNA	Deoxyribonucleic acid
dNTP	desoxynucleotide triphosphate
ECL	Enhanced chemiluminescence
EMT	Epithelial-mesenchymal transition
ER	Estrogen receptor
FBS	Fetal bovine serum
FN	Fibronectin
FPKM	Fragments per kilobase of exon per million fragments mapped
GBM	Glioblastoma multiforme
HR	Homologous recombination
HRP	Horseradish peroxidase
kDA	Kilo Dalton
miRNA	microRNA
MMR	Mismatch repair
NER	Nucleotide excision repair
NHEJ	Non-homologous end joining

PBS	Phosphate buffered saline
pre-miRNA	Precursor miRNA
pri-miRNA	Primary miRNA
PR	Progesterone receptor
PTEN	Phosphatase and tensin homolog
PTPN11	Protein tyrosine phosphatase, non-receptor type 11
p21	Cyclin-dependent kinase inhibitor 1A (CDKN1A)
P/S	Penicilllin/Streptomycin
qRT-PCR	Quantitative real time polymerase chain reaction
Rb	Retinoblastoma protein
SDS-PAGE	Sodium dodecyl sulfate polyacrylamide gel electrophoresis
Ser	Serine
TAE	Tris-acetate EDTA
TBST	Tris buffer saline Tween20
Thr	Threonine
TNBC	Triple-negative breast cancer
TNMK	Triple-negatif meme kanseri
TP53	Tumor protein 53
UTR	Untranslated region
ZEB1	Zinc finger e-box binding homeobox 1
ZEB2	Zinc finger e-box binding homeobox 2
ZO1	Zona occludens-1 (Tight junction protein 1, TJP1)

Chapter 1

Introduction

1.1. Breast cancer

After lung cancer, breast cancer is the second most common cancer and the leading cause of cancer associated deaths in women worldwide [1]. The global incidence rate of breast cancer is increasing dramatically as compared to other cancer types [2]. According to an estimation by American Cancer Society, approximately 250,000 women will be diagnosed with invasive breast cancer only in the US, of which 40,000 will die due to breast cancer in 2016 (American Cancer Society).

Breast cancer is a highly heterogeneous disease representing very distinct molecular, morphologic and clinical features. From clinical perspective, it encompasses 3 well-characterized sub-types based on the expression status of specific immunohistochemistry markers, namely, hormone receptors (estrogen receptor (ER) and progesterone receptor (PR)) and human epidermal growth factor receptor 2 (HER-2/ErbB2). These sub-types are 1.) hormone receptor positive (HR+) expressing higher levels of ER and PR, 2.) HER-2 positive (HER-2+) and, 3.) triple-negative breast cancer (TNBC) which lacks the expression of all three receptors [3, 4].

1.2. Subtype-dependent treatment of breast cancer

HR+ subtype accounts for a substantial number of breast cancers (around 70-80%). As these patients overexpress certain hormones, they are treated with hormone targeted therapies such as tamoxifen and aromatase inhibitors in clinics [5]. On the other hand, 20% of all breast cancer cases constitutes HER-2+ group in which HER-2 gene is amplified. Treatment of HER-2+

patients with HER-2 targeting monoclonal antibodies such as Trastuzumab (Herceptin) has shown to block tumor growth as well as to enhance chemotherapy response [6]. Lastly, TNBC, the most aggressive subtype of breast, cancer and it accounts for nearly 15% of all breast cancer population. As TNBC patients do not express any of 3 receptors, targeted-therapies cannot be utilized for the treatment. Therefore, chemotherapy is the mainstay treatment option for patients who are diagnosed with both early-stage and advanced-stage TNBC [7]. Among TNBC patients, only 30-40% patients respond to neoadjuvant chemotherapies (treatment prior to surgery) and the patients show up to 94% 5-year survival. The remaining TNBC patients initially respond towards certain chemotherapy agents but develop resistance over time. Due to aggressive relapse, 5-year survival rate is less than 60% in these TNBC patients [8]. As pathological complete response (pCR) is directly correlated with survival in TNBCs [9], it is necessary to improve the pCR rate to chemotherapies in these patients.

1.3. *BRCA1* and TNBC

Linkage analysis studies have led to the discovery of *BRCA1* gene as the first identified breast cancer susceptibility gene which is located at long (q) arm of chromosome 17 at position 21 (17q21) in human genome [10]. Mutations in this tumor suppressor gene have been found to be associated with high risk of breast and ovarian cancer onset [11]. *BRCA1* gene encodes very large proteins; specifically, one of the largest protein products of this gene is 1863 amino acid which is produced from 24 exons and is located in the nucleus of the cell [12]. BRCA1 contains 2 highly conserved functional domains: an N-terminal Ring domain and C-terminal BRCT domains. The Ring domain of BRCA1 possesses E3 ubiquitin ligase activity and is responsible for protein ubiquitination. The C-terminal BRCT domain of BRCA1 is a phospho-protein binding domain that has critical role in response to DNA damage [13, 14]. Mutations affecting cancer onset and progression have been found to be attributed mostly to these two domains, indicating their central role in genome integrity in breast and ovarian cancer [15, 16].

Approximately, 5 % of all breast cancer cases represents bearing pathogenic *BRCA1* mutations [17]. These breast cancer patients with *BRCA1* mutation mostly fall into TNBC subtype as they show similar morphologic features and immune-histochemical phenotypes (such as high expression of basal cellular markers and loss of tumor suppressor *PTEN*) attributable to a portion of TNBC (Figure 1.1). This subgroup of breast cancer, so-called basal-like breast cancer [18], also contains *TP53* mutations in general [19]. Although there are substantial similarities between TNBC and basal-like cancers, these groups are not fully identical to each other.

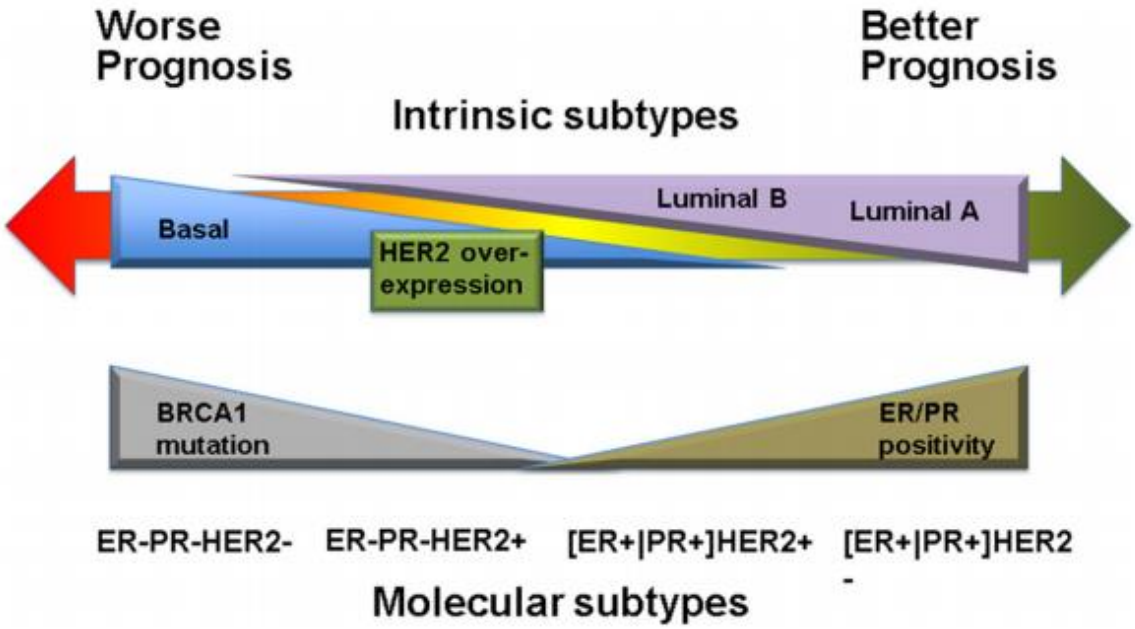

Figure 1.1. Schematic representation of breast cancer molecular subtypes based on patient outcome [20].

1.4. Treatment of *BRCA1*-mutated TNBCs with DNA cross-linking agents

Cisplatin is the first platinum-based chemotherapeutic agent that is used to treat many cancers. It causes a platinum complex formation which binds to DNA and triggers DNA cross-link. The resulting DNA damage leads to apoptosis when cells have insufficient DNA damage repair mechanisms [21].

Upon DNA damage, double-strand breaks are repaired via two major mechanisms: homologous recombination (HR) and non-homologous end joining (NHEJ). HR is a high-fidelity, less error-prone mechanism which uses a homologous sequence as template to resynthesize the DNA whereas NHEJ is more error prone mechanism as broken ends of DNA are clipped off during repair, but it is useful under circumstances where homologous template DNA for repair is not available. BRCA1 lies at the intersection of all DNA repair mechanisms and plays a major role in DNA repair through several mechanisms [22]. Loss of BRCA1 function renders cells hypersensitive to DNA damage and results in chromosomal aberrations when challenged with DNA damaging agents particularly platinum based inter-strand cross-linking agents [23]. Cisplatin treated cohort of *BRCA1*-mutated breast cancer had a significantly higher pCR rate as compared to treatment with non-platinum based individual or aggregated regimens [24, 25]. However, resistance development is inevitable in almost all cases. General mechanisms regulating platinum- based therapy resistance include elevated drug inactivation, increased DNA repair or DNA damage tolerance, improved expression of anti-apoptotic genes and inactivation of the p53 pathway [21]. Identification of molecular mechanisms involved in resistance development can help in improving the sensitivity of these *BRCA1*-mutated TNBC patients to platinum based regimens.

1.5. MicroRNAs

MicroRNAs (miRNAs) are small endogenous non-coding RNAs that are 20-25 nucleotides in length. They regulate gene expression at post-transcriptional level by targeting specific mRNAs through complementary base pairing preferentially in the 3'-UTR of target mRNAs and thus, lead to mRNA degradation and translational repression [26]. miRNAs are synthesized from primary miRNAs (pri-miRNAs) by RNase III-type proteins, Drosha and Dicer. By cleaving pri-miRNAs into ~70 nt long sequences, Drosha produces precursor miRNAs (pre-miRNAs) within the nucleus. Subsequently, pre-miRNAs are carried to the cytoplasm by exportin-5 (XPO5), where other RNase III endonuclease, Dicer, processes pre-miRNAs further into single stranded mature miRNAs which are then loaded onto RNA-induced silencing complex (RISC) together with Argonaute (ago) protein in order to perform mRNA downregulation by binding to seed-matching sequences in the 3′-UTR of mRNA (Figure 1.2) [27].

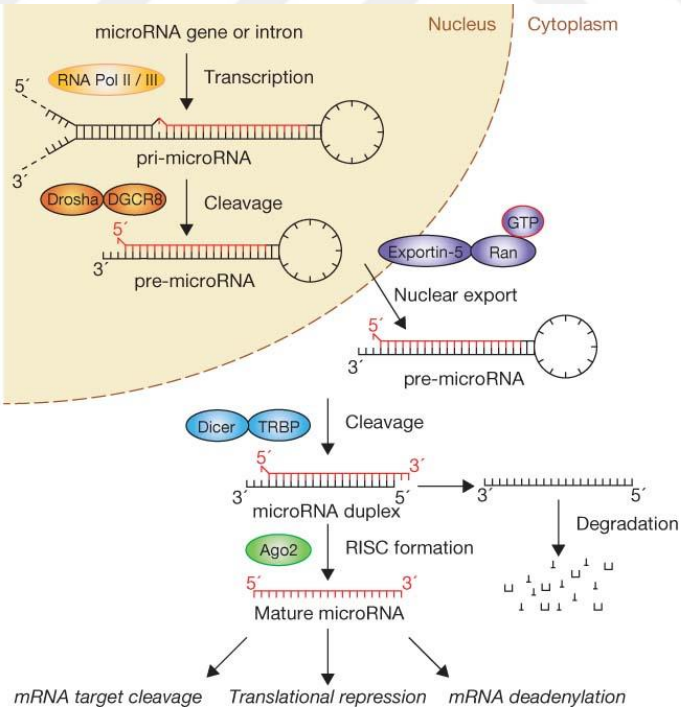

Figure 1.2. Schematic demonstration of miRNA biogenesis [28]. See Appendix for the copyright permission.

After the discovery of first animal microRNA more than 20 years ago, the number of miRNAs identified has been greatly expanded. So far, around 2600 miRNAs have been discovered in human genome [29], and that number increases with new studies using high-throughput sequencing [30]. Although they are tiny regulators of post-translational gene expression, their influence over genome regulation is huge. It is estimated that miRNAs are capable of controlling more than 60% of the human genome [31]. Recent scientific studies have showed that miRNAs play pivotal roles in many pathological processes such as epithelial-mesenchymal transition (EMT), metastasis and drug resistance in cancer [32]. In the context of drug resistance, for instance, our group showed that certain miRNAs regulate cell invasion and tamoxifen resistance [33] [34] [35]. Moreover, due to the fact that microRNAs can target more than one gene in a network manner [36], we also showed that it is more effective for cancer therapy to follow 'microRNA-protein interaction network' approach rather than conventional 'single microRNA-single protein' model [37]. In this regard, one study showed that miR-638 targets *BRCA1,* and its overexpression led to sensitization to DNA-damaging agents, ultraviolet (UV) and Cisplatin in TNBC cells [38]. However, there is no study indicating microRNAs role in *BRCA1*-mutated TNBC in a network manner.

1.6. MicroRNAs as drug candidates

The discovery that microRNAs function as crucial regulators of biological processes and their dysregulation in various human diseases is observed in common, therapeutic targeting of miRNAs is attracting scientists for novel therapy development in human pathologies [39]. A notable example for this is Miravirsen, an antisense oligonucleotide that binds to miR-122 and inhibits it in liver. This way hepatitis C virus (HCV) does not bound by miR-122 and therefore cannot replicate and multiply. After showing the effect of this modified miRNA oligonucleotide drug on HCV viremia in chimpanzees, Miravirsen is now being tested in human clinical trials

and was found to be safe with regard to toxicity [40]. On the other hand, miRNAs are promising anti-cancer agents as well. MRX34 is the first cancer therapy drug and encapsulated with liposomal nanoparticle formulation. It is a double-stranded mimic of miR-34, which is a tumor suppressor miRNA inhibiting oncogenicity and inducing cancer cell death [41]. In the Phase 1 clinical trial, MRX34 was found to have convincing results in different types of cancer including renal cell carcinoma, melanoma and hepatocellular carcinoma [42]. These clinical trials clearly demonstrate that miRNAs have high potential to be used as the therapeutic drugs without toxicity.

1.7. The rationale behind the study:

In this thesis, the aims are as following:

- Develop and validate acquired Cisplatin resistant cell line models of TNBC with *BRCA1* mutation
- Find out differentially expressed miRNAs and mRNAs in Cisplatin resistance using high-throughput miRNA/mRNA sequencing
- Construct miRNA-mRNA regulatory networks controlling Cisplatin resistance and unravel molecular targets to reverse this resistance

Chapter 2

Materials

2.1.. Buffers

1x Anode Buffer I	300mM Tris, 20% (v/v) methanol
1x Anode Buffer II	25mM Tris, 20% (v/v) methanol
1x Cathode Buffer	40mM 6-aminocaparoic acid, 20% (v/v) methanol
1x SDS-PAGE Running Buffer	25mMTris, 14.41g/l glycine, 1% (v/v) SDS
1x TAE	40mM Tris, 20mM acetic acid, 1mM EDTA
1x TBST	20nM Tris, 8g/l NaCl 0.2% (v/v) Tween20
RIPA lysis buffer	150mM NaCl, 1% (v/v) NP-40, 0.5% (v/v) Sodium DOC, 50mM TrisHCl (pH:8.0), 50mM NAF, 1mM NAVO4, 4% (v/v) Protease inhibitor, 4% (v/v) Phospatase inhitibor

2.2. Chemicals and Reagents

4x Protein Loading Dye	250mM Tris HCl (pH:6.8), 10% (w/v) SDS, 0.1% (w/v) Bromophenol blue,50% Glycerol (v/v), 25% (v/v) mercaptoethanol
6-aminocaparoic acid	Sigma Aldrich, St Louis, MO, USA
6x DNA loading Dye	New England Biolabds, Ipswich, MA, USA
Acetic acid	Sigma Aldrich, St Louis, MO, USA
Acrylamide/bisacrylamide	Applichem, Darmstadt, Germany
Agar	Sigma Aldrich, St Louis, MO, USA
Agarose	Promega, Madison, WI, USA

Ammonium peroxisulfate	Carlo Erba, Cornaredu, Italy
Bovine Serum Albumin	Santa Cruz, Dallas, TX, USA
Protease inhibitor cocktail	Roche Applied Science, Mannheim, Germany
dNTPs	Thermo Fisher Scientific, Waltham, MA, USA
ECL	Amersham Pharmacia Biotech, Amersham, UK
Ethanol	Sigma Aldrich, St Louis, MO, USA
Ethidium Bromide	Thermo Fisher Scientific, Waltham, MA, USA
Isopronapol	Sigma Aldrich, St Louis, MO, USA
LightCycler 480 SYBR Green I Master	Roche Applied Science, Mannheim, Germany
Lipofectamine 2000	Invitrogen, Carlsbad, CA, USA
Methanol	Sigma Aldrich, St Louis, MO, USA
Milk powder	Sigma Aldrich, St Louis, MO, USA
Nuclease free water	Applied Biosystems/Ambion, Austin, TX, USA
Page Ruler Protein Ladder	Thermo Fisher Scientific, Waltham, MA, USA
Phosstop	Roche Applied Science, Mannheim, Germany
Ponceu S	Sigma Aldrich, St Louis, MO, USA
Shandon Immu-mount	Thermo Fisher Scientific, Waltham, MA, USA
Sodium Chloride	Merck, Darmstandt, Germany
Sodium Dodecyl Sulfate (SDS)	Merck, Darmstandt, Germany
TEMED	Serva, Heidelberg, Germany
TRIsure	Bioline, Luckenwalde, Germany
Triton X-100	Sigma Aldrich, St Louis, MO, USA
Trizma base	Sigma Aldrich, St Louis, MO, USA
Trypton	Sigma Aldrich, St Louis, MO, USA

Tween-20	VWR, Radnor,PA, USA
Yeast Extract	Sigma Aldrich, St Louis, MO, USA

2.3. Enzymes and Enzyme Buffers

Phusion Polymerase	New England Biolabds, Ipswich, MA, USA
Taqman Abgene universal mix	Thermo Fisher Scientific, Waltham, MA, USA

2.4. Media and Supplements

DMEM	Lonza, Basel, Switzerland
Fetal bovine serum (FBS)	Biowest, Nuaille, France
Matrigel	BD, Flanklin Lakes, NJ, USA
Non-essential aminoacids	Lonza, Basel, Switzerland
optiMEM	Invitrogen, Carlsbad, CA, USA
Penicillin/streptomycin	Lonza, Basel, Switzerland

2.5. Kits

BCA Protein Assay Kit	Pierce, Rockford, IL, USA
Cell Titer-Glo cell viability assay kit	Promega, Madison, WI, USA
MycoAlert detection kit	Lonza, Basel, Switzerland
First strand cDNA synthesis kit	Fermantas, St. Leon-Roth, Germany
Taqman miRNA Assays	Applied Biosystems, Foster City, CA, USA

2.6. Equipments

Axiovision 4.3 microscopy	Carl Zeiss, Munich, Germany
Centrifuges	Thermo Fisher Scientific, Waltham, MA, USA
	Beckman, Pasadena, CA, USA
Cell culture hood	Nüve, Ankara, Turkey
Cell culture incubator	Nüve, Ankara, Turkey
Counting chamber	Marienfeld, Königshofen, Germany
Freezer (-80)	Hettich, Geldermansen, Holland
Freezer (-20)	Bosch, Stuttgart, Germany
Fridge	Bosch, Stuttgart, Germany
Horizontal Shakers	FinePCR, Seoul, South Korea
	Bellco, Vineland, NJ, USA
LightCycler 96	Roche Applied Science, Mannheim, Germany
Mini-PROTEAN Gel casting module	Biorad, Hercules, CA, USA
Mini-PROTEAN Tetra Cell	Biorad, Hercules, CA, USA
Multichannel Pipette	Thermo Fisher Scientific, Waltham, MA, USA
Nanodrop 1000	Thermo Fisher Scientific, Waltham, MA, USA
Nikon TS300 Inverted microscope	Nikon, Tokyo, Japan
PCR	Thermo Fisher Scientific, Waltham, MA, USA
Power supplies for electrophoresis	Biorad, Hercules, CA, USA
qPCR Machine	Roche Applied Science, Mannheim, Germany
Semidry western blot transfer unit	Biorad, Hercules, CA, USA
Synergy HT Multireader	Biotek, Winooski, VT, USA

UV-Reader	Vilber Lourmat, Eberhardzell, Germany
Vortex	Isolab, Wertheim, Germany
Water bath	Nüve, Ankara, Turkey
X-ray casette	Amersham Pharmacia Biotech, Amersham, UK
X-ray hyper processor	Amersham Pharmacia Biotech, Amersham, UK

2.7. Consumables

100mm dishes	Greiner bio-one, Frickenhausen, Germany
145mm dishes	Greiner bio-one, Frickenhausen, Germany
96-well plates	Greiner bio-one, Frickenhausen, Germany
6-well plates	Greiner bio-one, Frickenhausen, Germany
Filtered pipette tips (10ul, 20ul, 200ul, 1000ul)	Greiner bio-one, Frickenhausen, Germany
Cell scrapers	Greiner bio-one, Frickenhausen, Germany
Coverslips	Marienfeld, Königshofen, Germany
Cryovials	Greiner bio-one, Frickenhausen, Germany
Microscope slides	Marienfeld, Königshofen, Germany
Parafilm	VWR, Radnor,PA, USA
PCR tubes	Axygen, Corning, NY, USA
Plastic pipettes (10ml, 25ml)	Corning Incorporated, Corning, NY, USA
PVDF Membrane	Biorad, Hercules, CA, USA
Reaction tubes (500ul, 1.5ml, 2ml)	Axygen, Corning, NY, USA
Storage bottles (250ml, 500ml, 1L)	Corning Incorporated, Corning, NY, USA

Whatmann paper	GE Healthcare, Little Chalfont, UK
X-ray films	Kodak, Rochester, NY, USA
Cuvettes	VWR, Radnor,PA, USA
qPCR Plates	Roche Applied Science, Mannheim, Germany
White plates	Costar, Corning, NY, USA

Chapter 3

Methods

3.1 Culturing Human Breast Cancer Cell lines

HCC1937, MDA-MB-436, MDA-MB-231, and MCF-7 human breast cancer cell lines were obtained from American Type Culture Collection (Manassas, VA, USA). Cells were cultured in 100mm petri dishes at 37^{o}C 5% CO_2 condition. Cells were split two times per week in 1-to-3 ratio. For splitting cells were washed with 5ml PBS after culture media has been aspirated, trypsinized with 1.5ml trypsin in 37^{o}C for 5 minutes and re-suspended in appropriate culture medium. Dulbecco's Modified Eagle Medium (DMEM) with 10% Fetal Bovine Serum (FBS), 1% non-essential amino acids (NEAA) was used for the culture of the cells. All cell lines were tested for mycoplasma contamination periodically.

3.2. *In vitro* Cisplatin Resistant Cell Line Development

Resistance development in MDA-MB-436 cell line was started with 0.1 μM Cisplatin. When cells developed resistance to indicated dose, treatment dose increased to 0.25 μM Cisplatin. Likewise, with resistance, previous treatment dose was doubled to 0.5 μM Cisplatin. Finally, MDA-MB-436 cells became resistant to Cisplatin with 1 μM Cisplatin treatment dose as compared to wild-type cells in which vehicle treatment applied at the same time in order to prevent possible effects might be seen over time due to high passage number. HCC1937 cells, on the other hand, treated with 0.5 μM Cisplatin as a starting dose of resistance development. This amount increased to 1 μM, 2 μM, 4 μM and 5 μM as final resistance dose. As acquired resistance is dynamic process, in order not to reverse Cisplatin resistance MDA-MB-436 cells are being continuously treated with 1μM Cisplatin whereas the current treatment dose for HCC1937 is 5 μM.

3.3. miRNA mimics transfection and Cisplatin treatment

For transfection, cells were seeded 6000 cells/well for 96-well plates and 200,000 cells/well for 6-well plates with 100 ul or 2 ml penicillin/Streptomycin free (P/S-free) media respectively. Transfection of miR-455-3p and miR-455-5p mimics was performed using Lipofectamine 2000TM and OptiMEM.

24-hour after seeding miRNA mimic transfection was performed. For one well of 6-well format transfection, 2µl of lipofectamine was diluted in 250µl optiMEM and incubated at room temperature for 5 minutes after 20 seconds vortexing (mix A). For the same one well, miRNA mimics were also diluted in 250µl optiMEM simultaneously. Two vials (mix A and mix B) were mixed in 1:1 (v/v) ratio and vortexed for 15 seconds. Then, combined vial incubated at room temperature for 20 minutes and again vortexed for 15 seconds. After aspiration of media and addition of 1ml fresh P/S-free media on cells 500µl of transfection mixture was added on top of the cells resulting final volume of 1,5ml transfection medium. Cells were incubated at 37oC, 5% CO2 for further processes.

24-hour after miRNA mimic transfection Cisplatin treatment was applied to the cells. Like in the case of miRNA mimics transfection, required concentration of Cisplatin was prepared in 500µl of transfection medium and put on top of the cells. After Cisplatin administration cells were incubated 72-hour at 37oC, 5% CO2 to check cell viability or Western-Blot experiments.

3.4. *In vitro* viability

Cell Titer-Glo cell viability assay kit was used for the determination of cell viability. To do this, both reagent and cells in 96-well format incubated at room temperature for 30 minutes. After reaching the temperature equilibrium, Cell Titer-Glo reagent was administered to each well in a volume of 30 µl. Afterwards plate was placed to a shaker adjusted to high speed rotation (to ease cell lysis) for 10 minutes. Medium from each 96-well was transferred to corresponding wells of opaque white flat bottom 96-well plates and luminescence signal was measured on Biotek Multireader immediately. Percent viability for each replicate was calculated using Microsoft Excel (Albuquerque, NM, USA) and then graphics was drawn in GraphPad Prism. Student's two-tailed t-test was used for statistical analysis.

3.5. Sample preparation for RNA-Sequencing

Wild-type and Cisplatin-resistant cells were seeded in 10mm petri dishes and incubated at 27^{o}C 5% CO_2. After reaching 80-90 % confluency, they were washed with 1xPBS, trypsinized, collected in a 15 ml falcon tube and centrifuged at 1500 rpm for 5 minutes. For 2-times supernatant was discarded and pellet was washed with 1xPBS to ensure that all the media discarded. Afterwards the pellet was immediately placed to -80^{o}C until RNA isolation experiment performed. This procedure was repeated for 3 biological replicates for both wild-type and cisplatin-resistant cells. When all the pellets for each group obtained, total RNA isolated using TRISure reagent according to manufacturer's instructions. Total RNA was sent to McGill University Genome Center for both RNA-Sequencing and small-RNA-Sequencing.

3.6. RNA-Seq and small RNA Seq Analysis

Paired-end, 125 base-pair and rRNA-depleted stranded RNA Seq was done using Illumina HiSeq 2500. All the RNA-Seq analysis steps were conducted in UNIX command line environment from a desktop computer runs Linux operating system. Sequencing reads were

obtained as BAM files and first sorted according to name using samtools sort function. Name sorted BAM files for each condition were then converted to FASTQ reads using bedtools bamtofastq function. As aligner program that used this analysis (Tophat) requires indexed reference genome, reference genome sequences (GRCh38.p7.genome.fa) obtained in fasta format from GENCODE were indexed using bowtie2 build function. Using tophat2 version 2.1.1, raw fastq reads were mapped to reference genome with –g 1 option which allows only 1 multihits to a given reference sequence and therefore maps merely unique reads. To ease mapping step, known reference annotation and transcripts from GENCODE Release 25 (GRCh38.p7, gencode.v25.chr_patch_hapl_scaff.annotation.gtf) was included with –G function in the tophat code. Aligned RNA-Seq reads were then assembled and quantified with Cufflinks according to same annotation file used in Tophat mapping. Using Cuffmerge these assemblies were then merged together which provides a unique calculation of gene and transcript expression. The aligned reads and merged assembly were used as input for Cuffdiff which determines differentially expressed fatures and tests the statistical significance of these changes. CummeRbund tool which transforms the outputs of Cufflinks protocol into R statistical computer environment was used to plot graphics of RNA-Seq results.

For small RNA-Seq, size-selected small RNA-Seq libraries were sequenced in Illumina HiSeq 2000 machine. Single-end, 50 base-pair sequencing was performed. Sequencing reads obtained as BAM files were converted to FASTQ file format using bedtools bamtofastq function. Downstream analysis was done in a publicly available small RNA analysis tool called ‘sRNAtoolbox’. FASTQ reads for each condition were uploaded to the ‘sRNAbench’ module which performed adaptor trimming (Illumina RA3 adaptor sequence-TGGAATTCTCGGGTGCCAAGG), genome mapping (human hg19), and microRNA annotation and quantification based on miRBase annotation (Release 21). Obtained sRNAbench output files were then uploaded to ‘sRNA de’ platform which detects the

differentially expressed microRNAs. For the detection of differentially expressed samll RNAs it uses 3 widely accepted methods, edgeR, DEseq and NOISeq. In addition to the results of individual methods, it provides a consensus differential expression results. For this analysis, combination of edgeR and DESeq results were utilized for selecting differentially expressed miRNAs.

3.7. Ingenuity Pathway Analysis (IPA)

IPA version 01-07 was used to analyze differential expression data. Differential mRNA expression list as a Microsoft Excel file was uploaded to the system and analysis was performed with default parameters. Likewise differential miRNA expression list was uploaded and microRNA target filter feature used to find targets of the microRNAs. When considering the targets of the miRNAs, predictions were limited to differentially expressed mRNAs and 'expression pairing' function was applied. This way positively relugated mRNA targets of the miRNAs were eliminated. To construct the miRNA-mRNA networks, firstly, p53 network from IPA Upstream Regulator was displayed as network in IPA. Then, miRNAs were added to this network by considering target prediction algorithm consistency and expression base pairing with mRNAs. To have a clear picture of the network, indirect connections between the members of network were removed.

3.8. Quantitative Real-Time Polymerase Chain Reaction (qRT-PCR)

3.8.1. cDNA synthesis

RevertAid RT Reverse Transcription kit was used for reverse-transcription. 2ug total RNA from each sample was used to synthesize cDNA according to the protocol given at Table 3.1 and the reaction was incubated in thermocycler using the program given at Table 3.2.

Table 3.1. Components of reverse transcription reaction.

Reagent	**Concentration/Volume**
RNA	2µL (X µL)
oligoDT	1µL
5x Revert Aid reaction buffer	4µL
Ribolock Ribonuclease Inhibitor	1µL
dNTPs(10mM)	2µL
Revert Aid H Minus M-MuLV RT	1µL
H2O	(20-X) µL

Table 3.2. Thermocycler program for cDNA synthesis

Temperature	**Time**
37^{o}C	5 minutes
42^{o}C	60 minutes
70^{o}C	10 minutes
4^{o}C	∞

For qRT-PCR experiment, all samples were diluted to 1:10 after cDNA synthesis.

3.8.2. qRT-PCR for mRNA expression

For qRT-PCR, SYBR Green Master mix the primers listed on Table 3.3. were used.

Table 3.3. List of qRT-PCR primers

Name	Gene ID	Forward Primer	Reverse Primer
CDH1	999	5'-CCCGGGACAACGTTTATTAC-3'	5'-GCTGGCTCAAGTCAAAGTCC-3'
ZO1	7082	5'-CAGAGCCTTCTGATCATTCCA-3'	5'-CATCTCTACTCCGGAGACTGC-3'
FN	2335	5'-CTGGCCGAAAATACATTGTAAA-3'	5'-CCACAGTCGGGTCAGGAG-3'
SNAI2	6591	5'-TGGTTGCTTCAAGGACACAT-3'	5'-GTTGCAGTGAGGGCAAGAA-3'
ZEB1	6935	5'-GGGAGGAGCAGTGAAAGAGA-3'	5'-TTTCTTGCCCTTCCTTTCTG-3'
ZEB2	9839	5'-AAGCCAGGGACAGATCAGC-3'	5'-CCACACTCTGTGCATTTGAACT-3'
ACTB	60	5'-CCAACCGCGAGAAGATGA-3'	5'-CCAGAGGCGTACAGGGATAG-3'
HPRT	3251	5'-TGACCTTGATTTATTTTGCATACC-3'	5'-CGAGCAAGACGTTCAGTCCT-3'

qRT-PCR reaction was carried out in 96-well plate and a reaction mix was prepared for each primer pair (Table 3.4.). After addition of 8µl of mastermix, 2µg (final concentration of 20ng) of cDNA added separately into each well and carefully mixed by pipetting.

Table 3.4. Mastermix for qRT-PCR reaction

Reagent	Volume
SYBR Green	5µL
Forward Primer (20uM)	1µL
Reverse Primer (20uM)	1µL
H2O	1µL

Plate was tightly sealed, centrifuged at 1000rpm for 1minute at 4^{o}C before running on LightCycler® 96 qRT-PCR thermocycler (Roche Applied Science, Mannheim, Germany) with thermocycler program shown on Table 3.5.

Table 3.5. qRT-PCR program.

Pre-incubation							
Target (°C)	**Acquisition Mode**	**Hold (hh:mm:ss)**	**Ramp Rate (°C/s)**	**Acquisitions (per °C)**	**Sec Target (°C)**	**Step Size (°C)**	**Step Delay (cycles)**
95	None	00:05:00	4.4	5	0	0	0
Amplification							
Target (°C)	**Acquisition Mode**	**Hold (hh:mm:ss)**	**Ramp Rate (°C/s)**	**Acquisitions (per °C)**	**Sec Target (°C)**	**Step Size (°C)**	**Step Delay (cycles)**
95	None	00:00:10	4.4	5	0	0	0
58	Single	00:00:20	2.2	5	0	0	0
72	None	00:00:20	4.4	5	0	0	0
Melting Curve							
Target (°C)	**Acquisition Mode**	**Hold (hh:mm:ss)**	**Ramp Rate (°C/s)**	**Acquisitions (per °C)**	**Sec Target (°C)**	**Step Size (°C)**	**Step Delay (cycles)**
95	None	00:00:05	4.4	5	0	0	0
55	None	00:01:00	2.2	5	0	0	0
95	Continuous	00:00:00	0.11	5	0	0	0
Cooling							
Target (°C)	**Acquisition Mode**	**Hold (hh:mm:ss)**	**Ramp Rate (°C/s)**	**Acquisitions (per °C)**	**Sec Target (°C)**	**Step Size (°C)**	**Step Delay (cycles)**
40	None	00:00:30	2.2	5	0	0	0

3.8.3. Taqman qRT-PCR for miRNA expression

cDNA synthesis and qPCR for miRNAs were performed using AB Taqman miRNA Assays (Foster City, CA, USA). RT master mix was prepared using the materials shown in Table 3.6. Table 3.7. was used to perform miRNA reverse transcription.

Table 3.6. Mastermix for Taqman miRNA reaction

Reagent	**Volume for each 15µL reaction (µL)**
dNTPs (100nM)	0.15
MultiScribe TM Reverse Transcriptase (50U/µL)	1
10x RT Buffer	1.5
RNase Inhibitor (20U/µL)	0.19
Nuclease-free H_2O	4.16
Total	**7µL**

Table 3.7. PCR protocol for Taqman miRNA reverse transcription.

Temperature	**Time**
16^{o}C	30 minutes
42^{o}C	30 minutes
85^{o}C	5 minutes
4^{o}C	∞

For qPCR amplification of miRNA reverse transcription samples, Taqman 2x Master Mix was used as described in Table 3.8. 0.5µL of 20x Taqman miRNA ASsay mix (labeled as Real time) was added on top of 17.67 µL of PCR master mix for each well and 1.33µL of RT product for each sample was added into each well of 96-well qPCR opaque plates. After preparation of qPCR plate using 3 technical replicates for each experimental condition, PCR amplification was performed using PCR protocol on Table 3.9.

Table 3.8. Mastermix for Taqman miRNA PCR amplification.

Reagent	**Volume for each 20µL reaction (µL)**
Taqman 2X Universal PCR Master Mix	10
Nuclease-free H_2O	7.67
Total	**17.67**

Table 3.9. qPCR protocol for Taqman miRNA amplification.

<table>
<tr><th>Parameter</th><th colspan="4">Value</th></tr>
<tr><td>Run mode</td><td colspan="4">9600 emulation (Default)</td></tr>
<tr><td>Sample volume</td><td colspan="4">20µL</td></tr>
<tr><td rowspan="4">Thermal cycling parameters</td><td rowspan="3">Step</td><td>Type</td><td colspan="2">PCR</td></tr>
<tr><td rowspan="2">Hold</td><td colspan="2">40 cycles</td></tr>
<tr><td>Denature</td><td>Aneal</td></tr>
<tr><td>Time</td><td>10min</td><td>15sec</td><td>60sec</td></tr>
<tr><td>Temp (°C)</td><td>95</td><td>95</td><td>60</td></tr>
</table>

Auto Increment Settings	Accept default. (Default is 0.)
Ramp Rate Settings	Accept default. (Default is Standard.)
Data Collection	Accept default. (Default is 60^{o}C.)

3.9. Preotein Biochemistry

3.9.1. Protein Isolation

100,000 – 250,000 cells/well were seeded in 6-well plates and transfections (where indicated) were performed as mentioned previously. 24 hours later, indicated doses of Cisplatin were administered to the cells. After 72 hours of Cisplatin treatment, culture media was collected and centrifuged at 5000 rpm to pellet the apoptotic bodies. Cells were washed with 1ml 1XPBS and then trypsinized with 0.5-1 ml trypsin. 2-3 ml fresh media was added upon cell detachment, cell suspensions were collected carefully on top of apoptotic bodies and centrifuged at 1500 rpm to pellet the cells. Pelleted cells were washed with 3-5 ml 1X PBS and then re-centrifuged at same speed. Cell pellets were stored at -80 ^{o}C for further use. Depending on cell pellet size, 50-100 µL RIPA lysis buffer was added to the cells and mixed thoroughly by pipetting up and down. This RIPA suspension was transferred to 1.5 ml eppendorf tubes and vortexed for 5-10 seconds after every 5 minutes for a total of 20-30 minutes. Later, this suspension was centrifuged at 13000rpm 4^{o}C for 20 minutes. Supernatant was collected and stored at -20^{o}C for further experiments.

3.9.2. Protein Quantification

For protein quantification, BCA assay kit was used according to manufacturer's instructions. Range of 0-2µg/µL BSA standard solutions were prepared by serial dilution. Working solution was prepared by adding solution A and B in 50:1 ration and 200µL/well working solution was added pipetted into 96-well plate. Using dilution factor of 5 between standard and protein samples, 25µL of each standard and 5µL of each protein sample was pipetted in working solution in two replicates. After 30 minutes of incubation in 37ºC, absorbance was measured on SynergyHT microplate reader (Biotek, VT, USA) at 562nm. A standard calibration curve was drawn based on absorbance of BSA standards and sample concentrations were quantified from line graph of the curve.

3.9.3. Sodium dodecyl sulfate polyacrylamide gel electrophoresis (SDS-PAGE)

Concentrations of protein samples were equalized using 4X protein loading dye and samples were heated to 95ºC for 3-5 minutes. Polyacrylamide stacking and resolving gels were prepared according to Table 3.10.

Table 3.10. Mixture for stacking and resolving gels in different concentrations

Reagent	**8% Resolving gel**	**10% Resolving gel**	**12% Resolving gel**	**5% Stacking gel**
ddH2O	2.3ml	1.9ml	1.6ml	1.36ml
30% acrylamide mix	1.3ml	1.7ml	2ml	340µL

1 M Tris	(pH 8.8) 1.3ml	(pH 8.8) 1.3ml	(pH 8.8) 1.3ml	(pH 6.8) 260µL
10% SDS	50µL	50µL	50µL	20µL
10% APS	50µL	50µL	50µL	20µL
TEMED	5µL	5µL	5µL	2µL
Total volume	**5ml**	**5ml**	**5ml**	**2ml**

Firstly, Resolving gel solution was casted in the Biorad gel casting system and was overlaid with isopropanol until it is fully polymerized. Once polymerized, isopropanol was removed and stacking gel was casted on top of resolving gel and 10 or 15 well comb was placed in it. 15-20µg protein samples were loaded per well and empty wells were filled with diluted protein loading dye. Electrophoresis was performed at 110-130V for 90-120 minutes.

3.9.4. Western blotting

For semi-dry transfer, 3mm whatmann papers were cut in 7x9 cm^2 and 4 of them were moistened in anode buffer-I, 2 of them in anode buffer-II and 6 of them in cathode buffer. PVDF membrane was first dipped in 100% methanol for 3 minutes and then in anode buffer II for 1 minute. 4 anode I, 2 anode II, PVDF membrane, stacking gel, 6 cathode papers were stacked from anode to cathode in Semi-dry Turbo Blot machine. Transfer was performed at 25V for 30 minutes.

After transfer, PVDF membrane was stained with Ponceu S solution for 3 minutes and washed with ddH_2O until ponceu stain was completely removed. Membranes were cut at specific kDa

of interest and blocked with 5% (w/v) milk:1X TBS-T or 5% (w/v) BSA:1X TBS-T for 1 hour at room temperature on slow shaking. Later, blocking solution was removed and membranes were incubated in primary antibody either for 1-hour at room temperature or overnight at 4ºC (Table 3.11).

Table 3.11. List of primary and secondary antibodies used in western blot.

Gene Name	**Firm**	**Catalog Number**	**Dilution**
Beta-actin	MP Biomedicals	69100	1:5000
Cleaved Caspase 3	Cell Signaling Technology	CST9664S	1:1000
Phospho-Histone H2AX (Ser139)	Cell Signaling Technology	9718	1:1000
HRP-coupled anti-rabbit IgG	Cell Signaling Technology	CST7074	1:10000
HRP-coupled anti-mouse IgG	Cell Signaling Technology	CST7076	1:10000

After primary antibody incubation, membranes were washed with 1X TBS-T thrice for 10 minutes on shaker. Membranes were then incubated in secondary antibody either for 1-hour at room temperature or overnight at 4ºC. After secondary antibody incubation, membranes were again washed with 1X TBS-T thrice for 10 minutes on shaker. After washing, membranes were placed on X-ray cassette and ECL reagents, mixed in 1:1 ratio, were applied to membrane. In dark, X-ray films were exposed to membranes for different time periods ranging from 3 seconds to 30 minutes and then developed.

Chapter 4

Results

4.1. Development and characterization of Cisplatin resistant TNBC cell line models having *BRCA1* mutation

Cancer-associated *BRCA1* mutations lead to less expressed protein product that unable to sensor DNA damage and initiate repair mechanisms resulting in cell death [43]. As *BRCA1* has crucial role in repairing double-stranded DNA damage, Cisplatin response in TNBC cell lines where *BRCA1* is wild-type (MDA-MB-231) or mutated (MDA-MB-436 and HCC1937) was investigated. In line with the previous literature findings [44], mutation in *BRCA1* gene leading to insufficient DNA damage repair resulted in lower IC50 values in MDA-MB-436 and HCC1937 cells as compared to that of *BRCA1* wild-type MDA-MB-231 cells (Figure 4.1). This effect is not peculiar only to TNBC cells as MCF-7, an ER+ breast cancer cell line, showed almost no response to Cisplatin. Overall, these findings showed that *BRCA1*-mutated TNBC cell lines are more sensitive to Cisplatin as compared to *BRCA1* wild-type TNBC and ER+ cell lines as expected and used as our models for developing Cisplatin-resistant TNBC cell lines with *BRCA1* mutation.

A

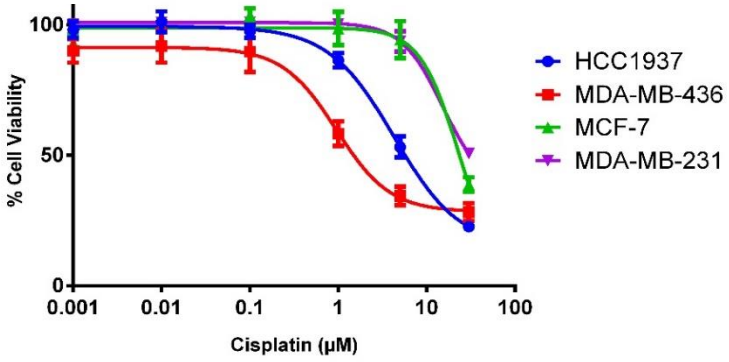

B

Cell Line	IC50 (μM)
MDA-MB-436	0.9475
HCC1937	4.281
MDA-MB-231	15.25
MCF-7	~ 22.93

Figure 4.1. Cell Titer Glo cell viability assay results for HCC1937, MDA-MB-436, MDA-MB-231 and MCF-7 cells. **A.** Dose-response curve showing the Cisplatin response of the indicated cells. **B.** Table shows the IC50 values for Cisplatin in each cell line.

Despite having initial response to Cisplatin, most of the patients develop Cisplatin resistance over time in various types of cancer [45] [46] [47]. To mimic acquired Cisplatin resistance observed in patients, we developed *in vitro* Cisplatin resistant *BRCA1*-mutated TNBC cell lines. To do this, these cell lines were exposed to gradually increasing doses of Cisplatin for 9 months (Figure 4.2). Resistance development was verified with Cell Titer Glo Cell viability assay. Results clearly demonstrate that both cell lines have acquired Cisplatin resistance and importantly stayed as resistant during our experimental work (Figure 4.3).

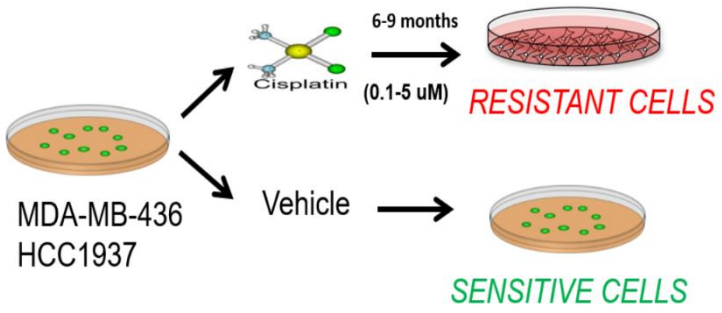

Figure 4.2. Graphical representation of *in vitro* Cisplatin resistance development**.** MDA-MB-436 cells exposed to Cisplatin doses ranging from 0.1-1 μM whereas HCC1937 cells were

treated with 0.5-5 μM Cisplatin for 9 months. During that time sensitive cells were passaged along with resistant cells.

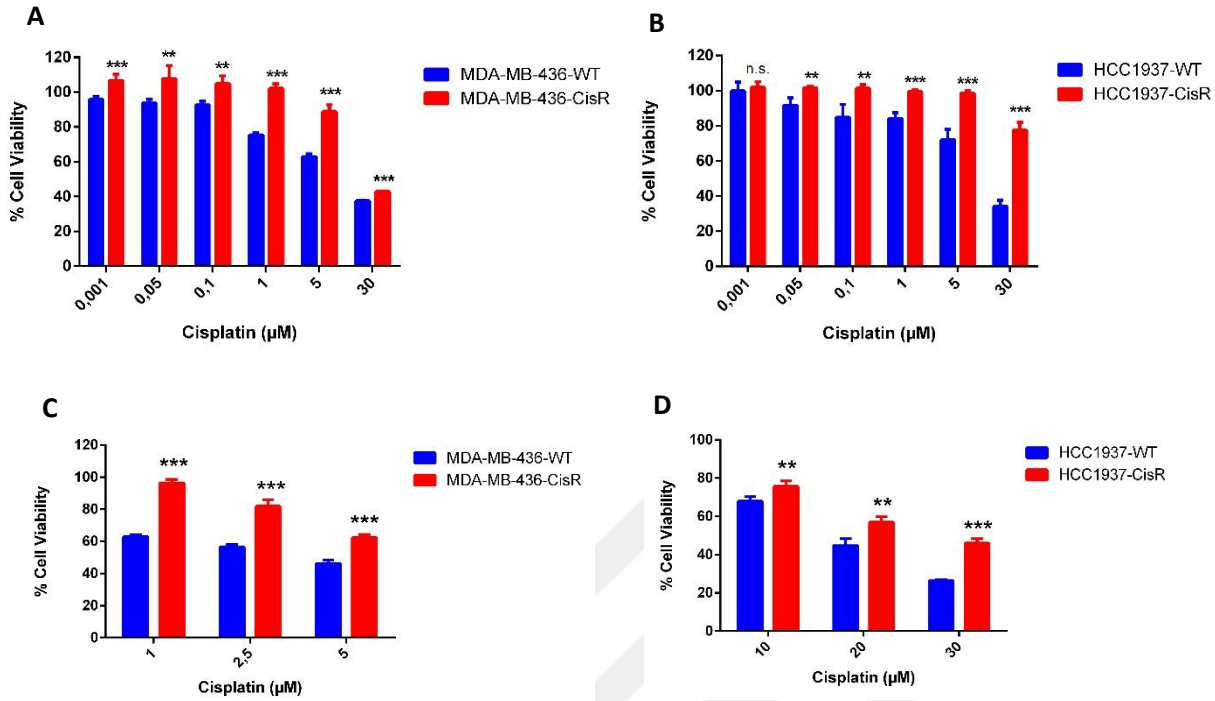

Figure 4.3. Cell Titer Glo cell viability assay results of MDA-MB-436-WT, MDA-MB-436-CisR and HCC1937-WT, HCC1937-CisR cells. **A and B**. Bar graphs showing Cisplatin response for sensitive and resistant cells after 9 months of drug exposure. **C and D**. The same as A and B, but viability assay was performed 15 months later.

4.2. Genomic characterization of Cisplatin resistance by miRNA-mRNA sequencing

In order to determine differentially expressed miRNAs in Cisplatin resistant *BRCA1* mutated TNBC cells, small RNA-seq was performed using RNA samples from 3 biological replicates of *wild-type* and Cisplatin-resistant cell lines. Sequencing reads were analyzed with 'sRNA toolbox' which is a publicly available small RNA-Seq data analysis platform (Figure 4.4) [48]. Using consensus results obtained from deSeq and edgeR algorithms, we defined differentially expressed miRNAs that are commonly deregulated in both cell lines. In total 32 miRNAs were found to be significantly (adjusted p-value less than 0.05) deregulated in Cisplatin resistance,

of which 25 miRNAs were downregulated and 7 miRNAs was upregulated in both MDA-MB-436-CisR and HCC1937-CisR cells (Figure 4.5 and Table 4.1).

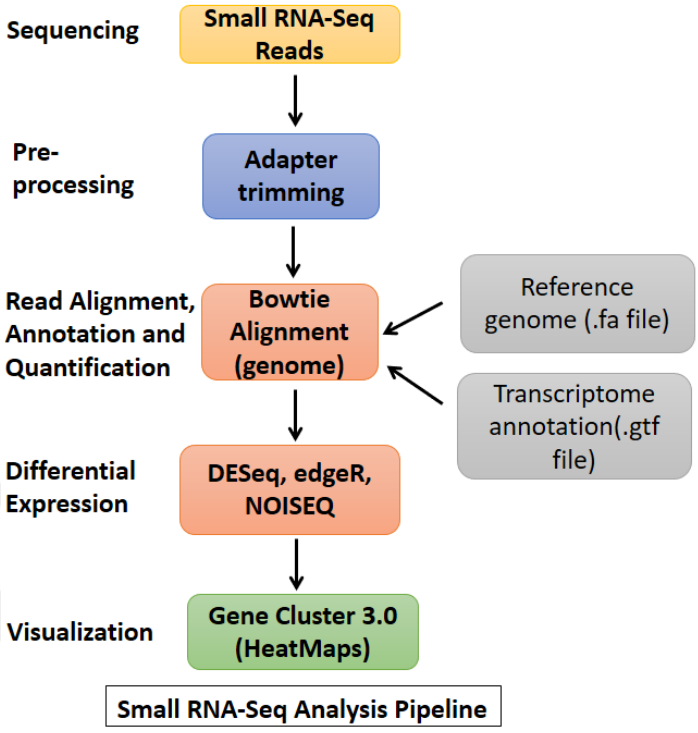

Figure 4.4. sRNA toolbox small RNA-Seq analysis pipeline.

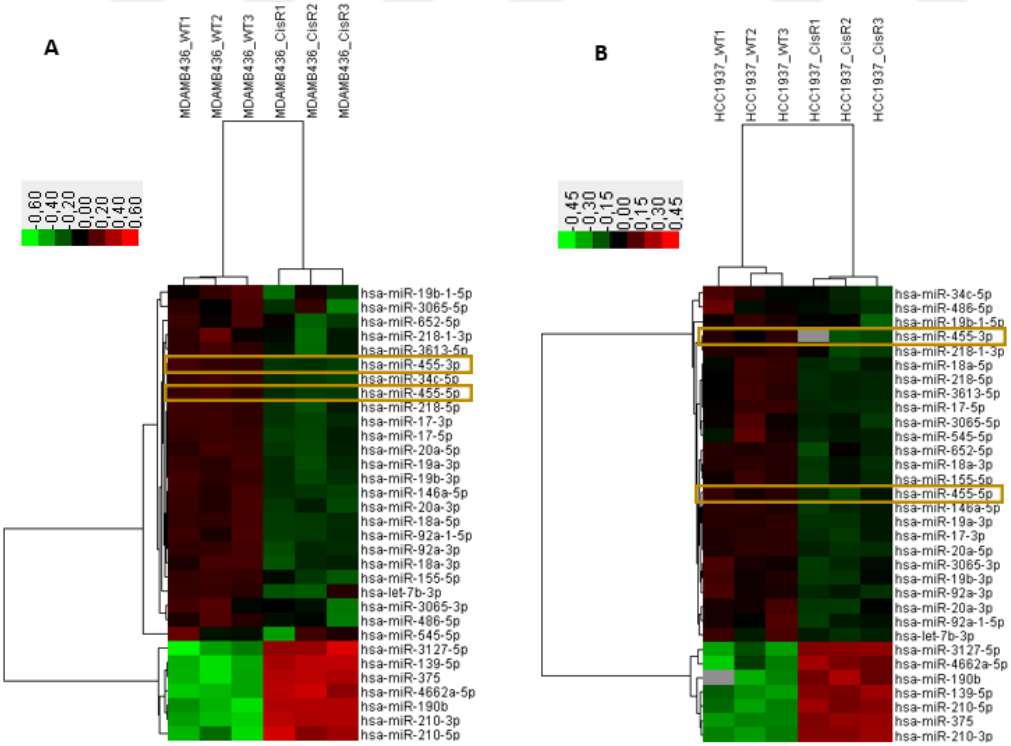

Figure 4.5. Heatmaps showing most differentially expressed miRNAs in both MDA-MB-436-CisR (**A**) and HCC1937-CisR cells (**B**). miR-455-3p and miR-455-5p were highlighted in yellow rectangulars.

	MDA-MB-436-CisR		HCC1937-CisR	
miRNA	log2FC	padj	log2FC	padj
hsa-miR-34c-5p	-6.414	5.183E-250	-0.609	2.361E-02
hsa-miR-146a-5p	-3.980	7.695E-33	-0.726	7.129E-04
hsa-miR-455-3p	-1.973	2.029E-38	-3.923	6.484E-07
hsa-miR-218-1-3p	-1.697	1.644E-05	-2.998	6.587E-06
hsa-miR-455-5p	-1.626	5.241E-31	-2.010	6.835E-07
hsa-miR-652-5p	-1.452	3.173E-07	-1.276	1.984E-04
hsa-miR-19b-1-5p	-1.391	3.173E-07	-1.665	1.335E-04
hsa-miR-20a-3p	-1.343	3.787E-13	-1.308	5.903E-05
hsa-miR-18a-5p	-1.314	9.872E-27	-1.597	3.672E-08
hsa-miR-218-5p	-1.232	5.417E-24	-1.571	3.180E-10
hsa-miR-3613-5p	-1.221	1.514E-13	-1.027	1.777E-03
hsa-miR-3065-3p	-1.209	2.212E-04	-1.508	3.371E-06
hsa-miR-17-5p	-1.199	4.854E-40	-1.312	2.144E-15
hsa-miR-19a-3p	-1.183	3.649E-25	-1.408	1.509E-09
hsa-miR-3065-5p	-1.127	3.446E-03	-1.781	1.080E-04
hsa-miR-18a-3p	-1.102	1.078E-12	-1.492	4.002E-06
hsa-miR-20a-5p	-1.085	7.184E-34	-1.411	1.009E-18
hsa-miR-155-5p	-1.048	8.962E-17	-2.175	9.417E-17
hsa-miR-17-3p	-1.043	9.554E-17	-1.392	7.714E-08
hsa-miR-92a-3p	-1.012	1.307E-58	-1.128	1.087E-08
hsa-miR-92a-1-5p	-0.942	3.025E-09	-2.798	3.242E-03
hsa-miR-19b-3p	-0.938	1.008E-21	-1.186	9.876E-11
hsa-miR-545-5p	-0.811	3.149E-02	-1.109	2.266E-03
hsa-miR-486-5p	-0.785	1.549E-08	-0.847	7.793E-03
hsa-let-7b-3p	-0.765	4.386E-07	-0.894	2.718E-04
hsa-miR-139-5p	2.850	4.487E-48	2.327	4.450E-05
hsa-miR-375	2.003	3.569E-29	1.509	2.652E-11
hsa-miR-3127-5p	1.361	1.305E-03	0.842	3.725E-02
hsa-miR-190b	1.068	1.496E-02	2.120	1.405E-03
hsa-miR-4662a-5p	0.746	6.557E-05	1.713	3.772E-03
hsa-miR-210-5p	0.639	7.396E-03	1.465	6.288E-06
hsa-miR-210-3p	0.608	9.553E-06	1.222	8.946E-08

Table 4.1. Table showing most differentially expressed miRNAs in Cisplatin resistant cells.

4.3. miR-455-3p and miR-455-5 are highly downregulated in both Cisplatin resistant models, and their overexpression leads to sensitization to Cisplatin

miR-455-3p and miR-455-5p, which are the most highly downregulated miRNAs in both Cisplatin resistant cell lines, were selected for further analysis (Figure 4.5 and Table 4.1). Firstly, we examined the expression levels of these miRNAs in our Cisplatin resistant models

using miRNA TaqMan. In concordance with the sequencing results, both miR-455-3p and miR-455-5p were significantly downregulated in resistant cells as compared to their wild-type counterparts in both Cisplatin resistant cell line models (Figure 4.6).

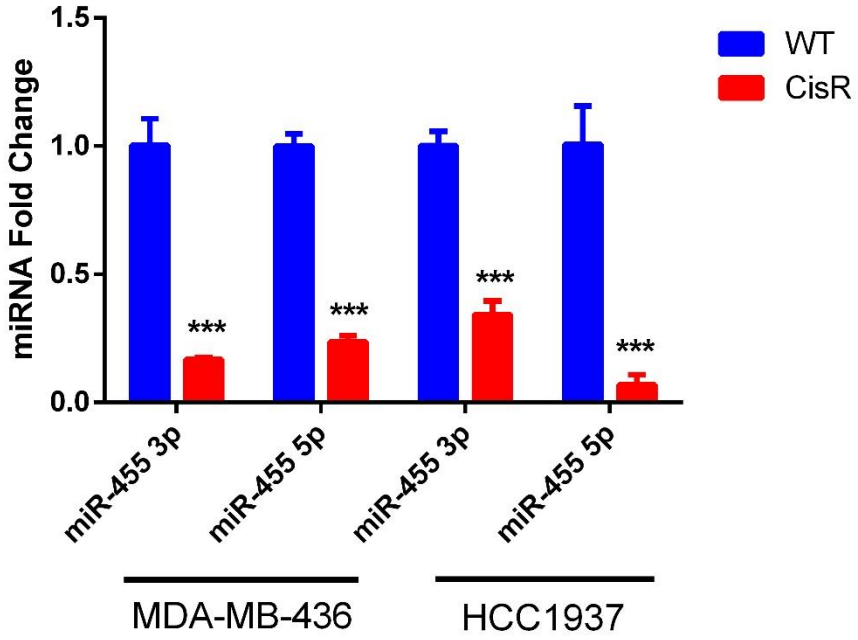

Figure 4.6. Taqman qRT-PCR results showing the miR-455-3p and miR-455-5p expression levels in Cisplatin sensitive and resistant cells. RNU44 was used as a housekeeping control (n=4).

After validating downregulation of the miRNAs in the resistant state, we checked whether their upregulation *via* miRNA mimic transfections in the presence of Cisplatin could sensitize resistant cells to the drug. In line with sequencing results, both miRNAs showed Cisplatin sensitization effect (Figure 4.7).

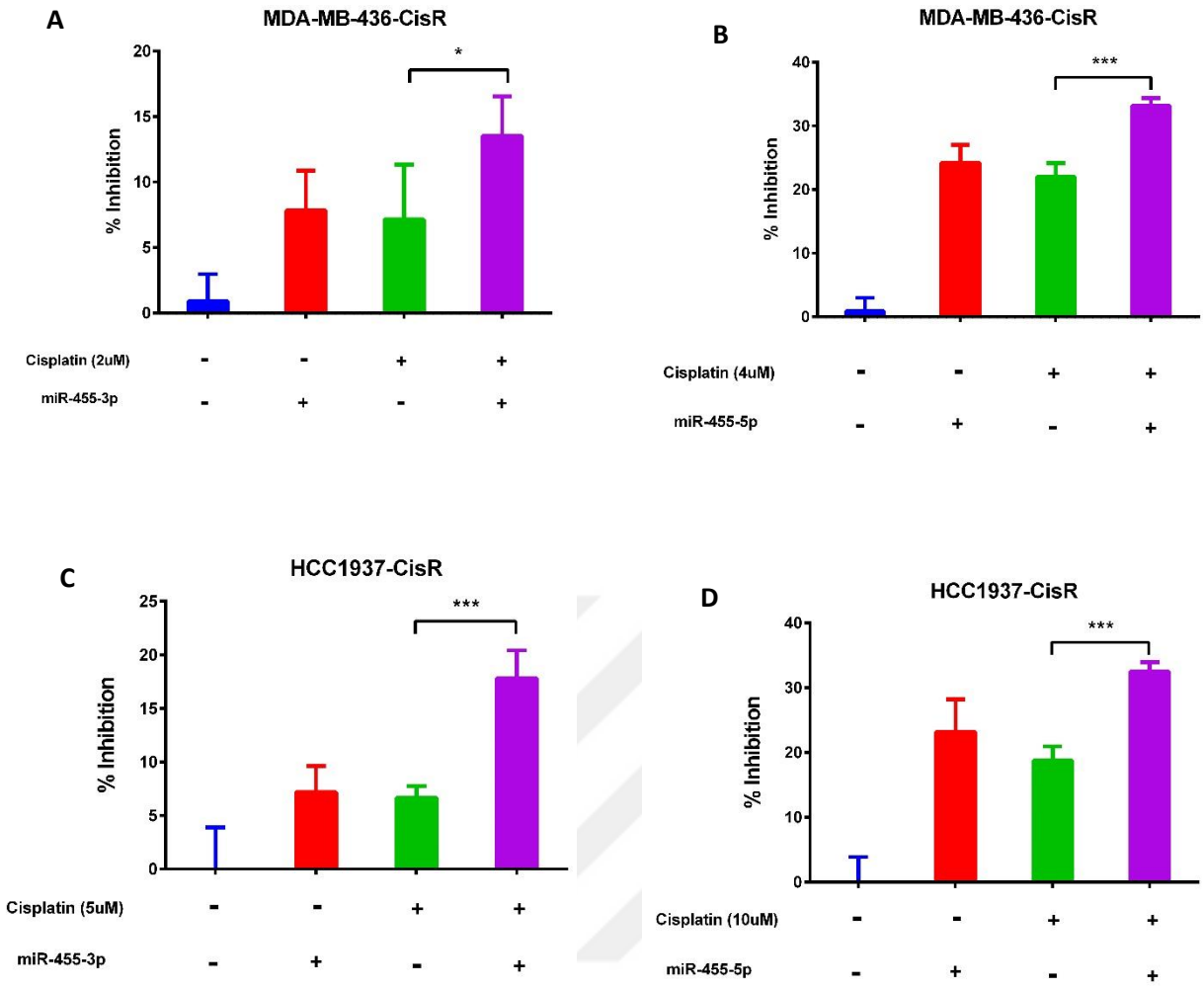

Figure 4.7. Bar graphs showing miR-455-3p and miR-455-5p impact on Cisplatin response. Changes in cell viability inhibition in MDA-MB-436-CisR cells transfected with/without miR-455-3p and treated with/without 2 µM Cisplatin (**A**) or in the same cells transfected with/without miR-455-5p and treated with/without 4 µM Cisplatin (**B**) or in HCC1937-CisR cells transfected with/without miR-455-3p and treated with/without 5 µM Cisplatin (**C**) or in the same cells transfected with/without miR-455-5p and treated with/without 10 µM Cisplatin (**D**).

4.4. Overexpression of miR-455-3p, but not that of miR-455-5p, leads to increased cleaved Caspase-3 and p-H2AX

To examine whether decrease in proliferation is due to apoptosis, we performed Western-Blot using a well-known apoptosis marker, cleaved caspase-3 [49]. When miR-455-3p mimic combined with Cisplatin, more apoptosis was observed as compared to Cisplatin treatment alone in MDA-MB-436-CisR and HCC1937-CisR cell lines. We observed very dramatic increase in apoptosis when using Cisplatin plus miR-455-5p in HCC1937-CisR cells. However, miR-455-5p and Cisplatin combination did not lead to an increase in apoptosis for MDA-MB-436-CisR cells. Phosphorylation of histone H2AX is a marker for DNA damage and more specifically related to presence of double-stranded breaks [50]. To test if the sensitization accompanied by apoptosis for miR-455-3p mimic along with Cisplatin leads to augmented p-H2AX protein level indicating double-stranded break accumulation without proper repair and consequent apoptosis, we examined the level of p-H2AX upon miR-455 overexpression in the presence of Cisplatin. We observed that miR-455-3p along with Cisplatin leads to an increase in p-H2AX; however, this was not the case for miR-455-5p. Even p-H2AX level decreased in the combination regimen, suggesting an alternative regulatory mechanism for sensitization effect other than DNA-damage response-related apoptosis (Figure 4.8).

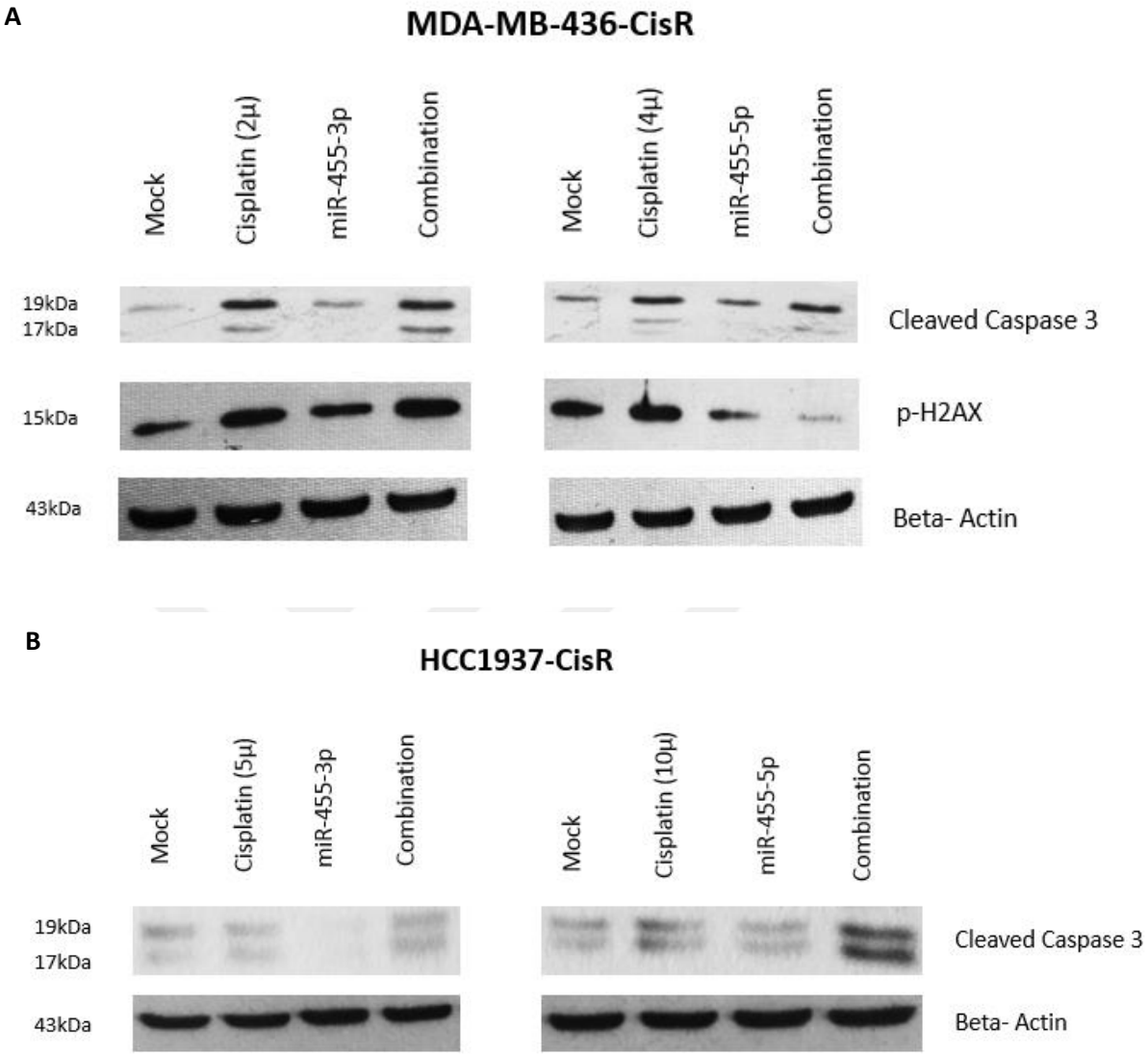

Figure 4.8. Western Blot analysis showing cleaved caspase-3 and p-H2AX protein levels in MDA-MB-436-CisR cells treated with i) 2 μM Cisplatin or 20 nM miR-455-3p or combination of 2 μM Cisplatin and 20 nM miR-455-3p or ii) 4 μM Cisplatin or 20 nM miR-455-5p or combination of 4 μM Cisplatin and 20 nM miR-455-5p (**A**). Western Blot analysis showing cleaved caspase-3 protein levels in HCC1937-CisR cells treated with i) 5 μM Cisplatin or 20 nM miR-455-3p or combination of 5 μM Cisplatin and 20 nM miR-455-3p ii) 10 μM Cisplatin or 20 nM miR-455-5p or combination of 5 μM Cisplatin and 20 nM miR-455-5p (**B**).

4.5. RNA-Seq analysis to construct global miRNA-mRNA networks and identify potential targets of miR-455-3p and miR-455-5p

To construct the global miRNA-mRNA network and also to find the target mRNAs of candidate miRNAs, (miR-455-3p and miR-455-5p), whole transcriptome RNA-Sequencing was done. Sequencing results were analyzed using a well-established protocol [51] (Figure 4.9).

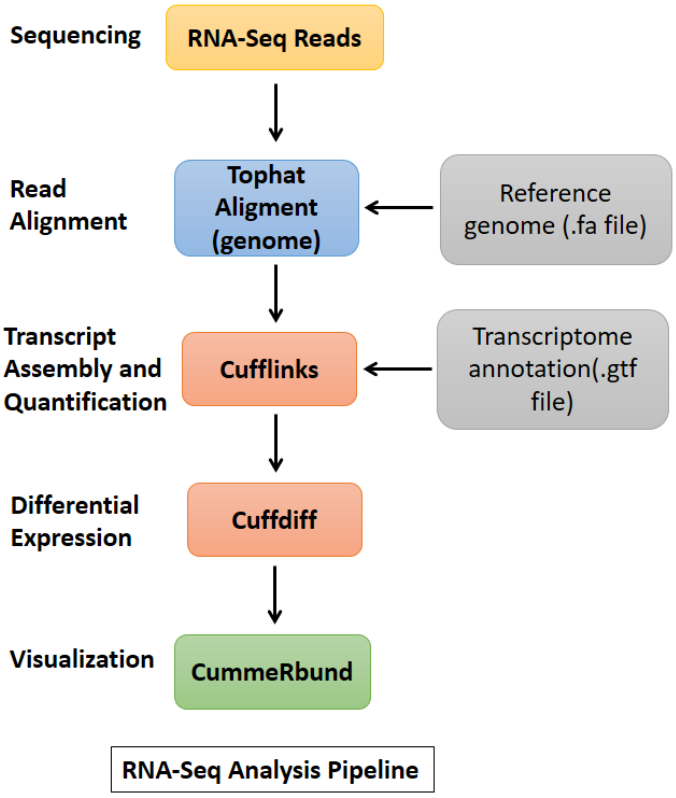

Figure 4.9. Graphical representation of RNA-Seq analysis pipeline.

Regarding the evaluation of RNA-Seq data quality, the squared coefficient of variation (CV^2) is an important parameter. CV^2 is a normalized measure of variability observed across replicates. The more CV^2 differ between experimental conditions, the less differentially expressed genes are detected. That is because there is high amount of variability between

replicate fragments per kilobase of exon per million fragments mapped (FPKM) estimates. As seen from Figure 4.10, differences in CV^2 are less between MDA-MB-436 and MDA-MB-436-CisR as compared to HCC1937-WT and HCC1937-CisR, resulting in presence of more differentially expressed genes.

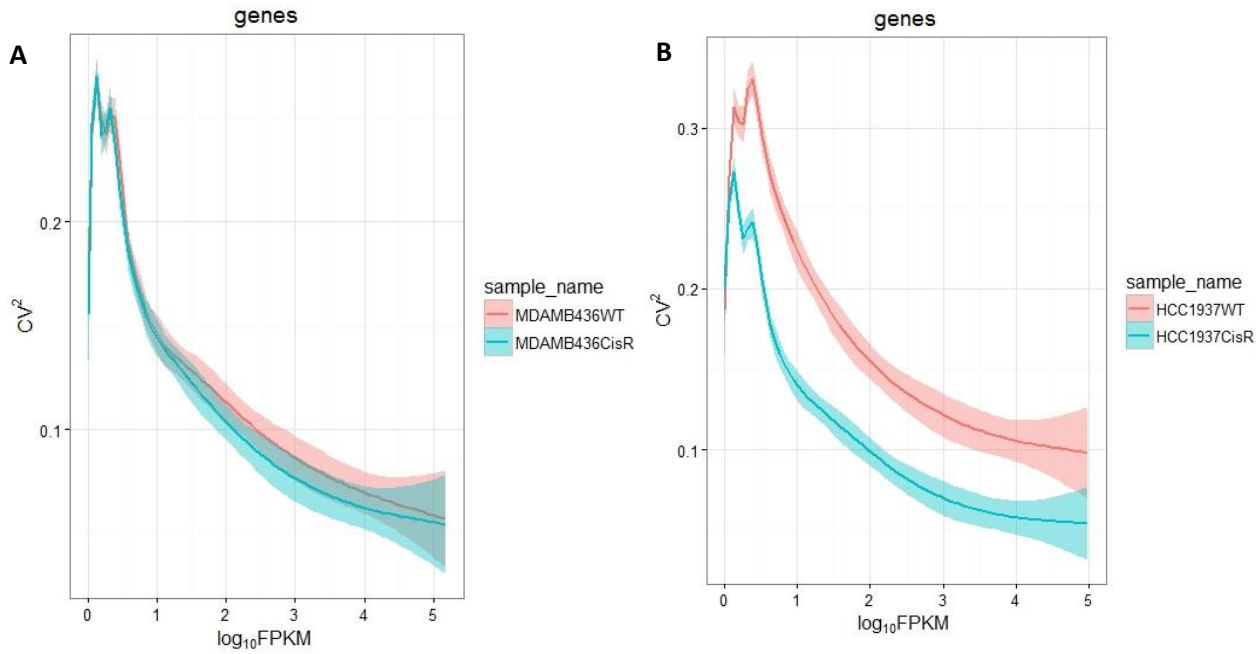

Figure 4.10. The squared coefficient of variance (SCV) plots showing log_{10}FPKM values in the x axis and CV^2 values in the y axis in MDA-MB-436 model (**A**) and in HCC1937 model (**B**). Red colour indicates wild type (WT) and blue colour indicates Cisplatin resistant (CisR) groups of both models.

Concerning distribution of the counts, boxplots are useful visualization tools. In figure 4.11, boxplots show the log_{10} (FPKM) scores between the samples in both resistant models. Besides, the distributions of FPKM values which might give insight into the global amount of downregulated and upregulated genes were illustrated with density plots (Figure 4.11).

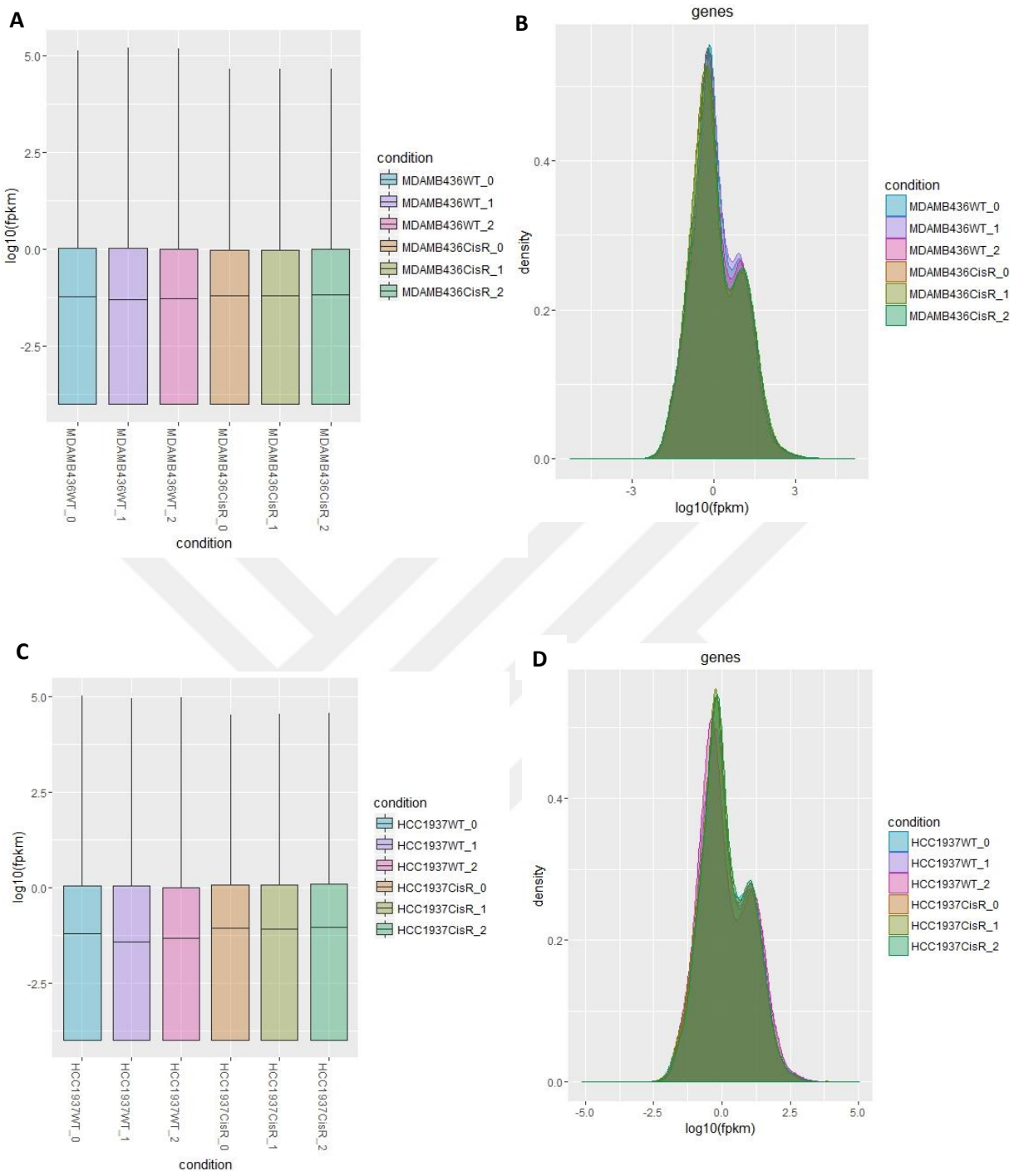

Figure 4.11. Boxplots showing $\log_{10}$ (FPKM) values in MDA-MB-436 model (**A**) and HCC1937 model (**C**). Density plots showing $\log_{10}$ (FPKM) scores among groups in MDA-MB-436 model (**B**) and and HCC1937 model (**D**).

To display correlation between groups, pairwise scatterplots were drawn. As expected, wild-type and resistant cases correlated within wild-type and resistant groups, respectively (Figure 4.12).

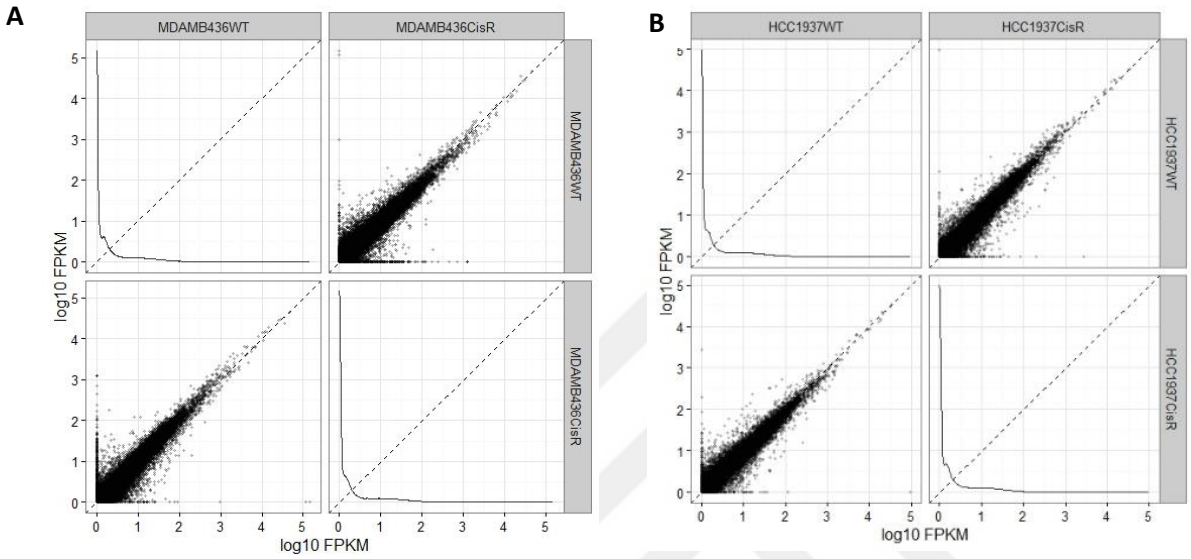

Figure 4.12. Pariwise scatter plots illustrating correlation analysis between groups by comparing $\log_{10}$ (FPKM) values within wild-type and resistant groups of MDA-MB-436 (**A**) and HCC1937 (**B**).

Similarities between replicates can be very useful for determining the relationship between conditions and therefore identifying outlayers. To this end, dendograms were used to illustrate clustering of genes. Accordingly, *wild-type* and resistant samples clustered together in dendogram trees. Likewise, distance matrixes gave similar results with dendograms (Figure 4.13).

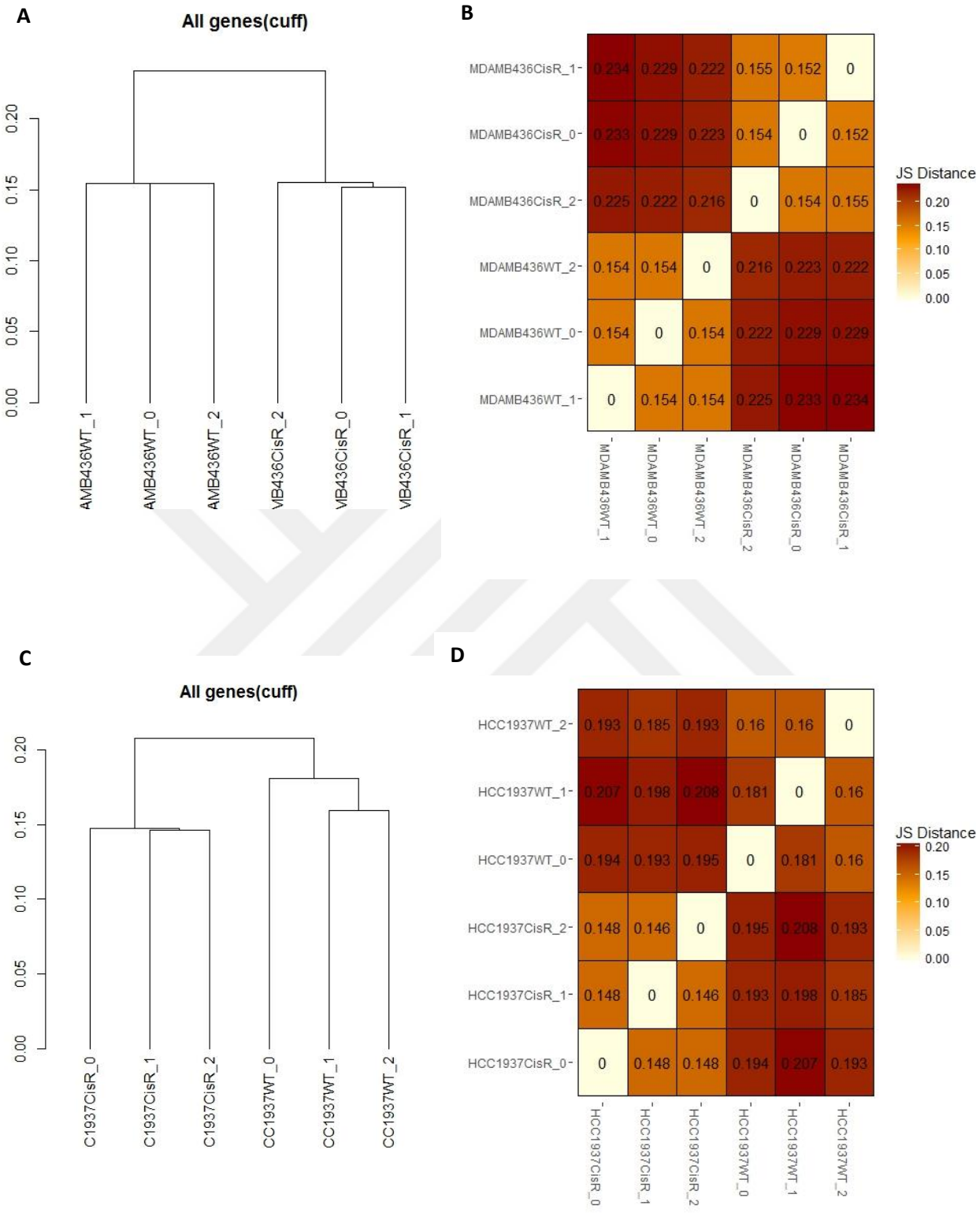
A
All genes(cuff)
0.00
0.05
0.10
0.15
0.20
AMB436WT_1
AMB436WT_0
AMB436WT_2
MB436CisR_2
MB436CisR_0
MB436CisR_1
B
MDAMB436CisR_1
MDAMB436CisR_0
MDAMB436CisR_2
MDAMB436WT_2
MDAMB436WT_0
MDAMB436WT_1
0.234 0.229 0.222 0.155 0.152 0
0.233 0.229 0.223 0.154 0 0.152
0.225 0.222 0.216 0 0.154 0.155
0.154 0.154 0 0.216 0.223 0.222
0.154 0 0.154 0.222 0.229 0.229
0 0.154 0.154 0.225 0.233 0.234
JS Distance
0.20
0.15
0.10
0.05
0.00
C
All genes(cuff)
0.00
0.05
0.10
0.15
0.20
C1937CisR_0
C1937CisR_1
C1937CisR_2
CC1937WT_0
CC1937WT_1
CC1937WT_2
D
HCC1937WT_2
HCC1937WT_1
HCC1937WT_0
HCC1937CisR_2
HCC1937CisR_1
HCC1937CisR_0
0.193 0.185 0.193 0.16 0.16 0
0.207 0.198 0.208 0.181 0 0.16
0.194 0.193 0.195 0 0.181 0.16
0.148 0.146 0 0.195 0.208 0.193
0.148 0 0.146 0.193 0.198 0.185
0 0.148 0.148 0.194 0.207 0.193
JS Distance
0.20
0.15
0.10
0.05
0.00

Figure 4.13. Dendograms showing clustering of the replicates within the groups in MDA-MB-436 cells (**A**) and HCC1937 cells (**C**). Distance matrixes showing the correlation between the groups in MDA-MB-436 cells (**B**) and HCC1937 cells (**D**).

Moreover, dimensionality reduction is an another method for clustering of the groups and identifying the variability and connection/correlation between conditions. For this purpose, cummeRbund has integrated 2 types of dimensionality reduction method: Principal Component Analysis (PCA) and Multi-Dimensional Scaling (MDS). In line with previous clustering and variability results, both *wild-type* and resistant cells can be easily discriminated from each other (Figure 4.14).

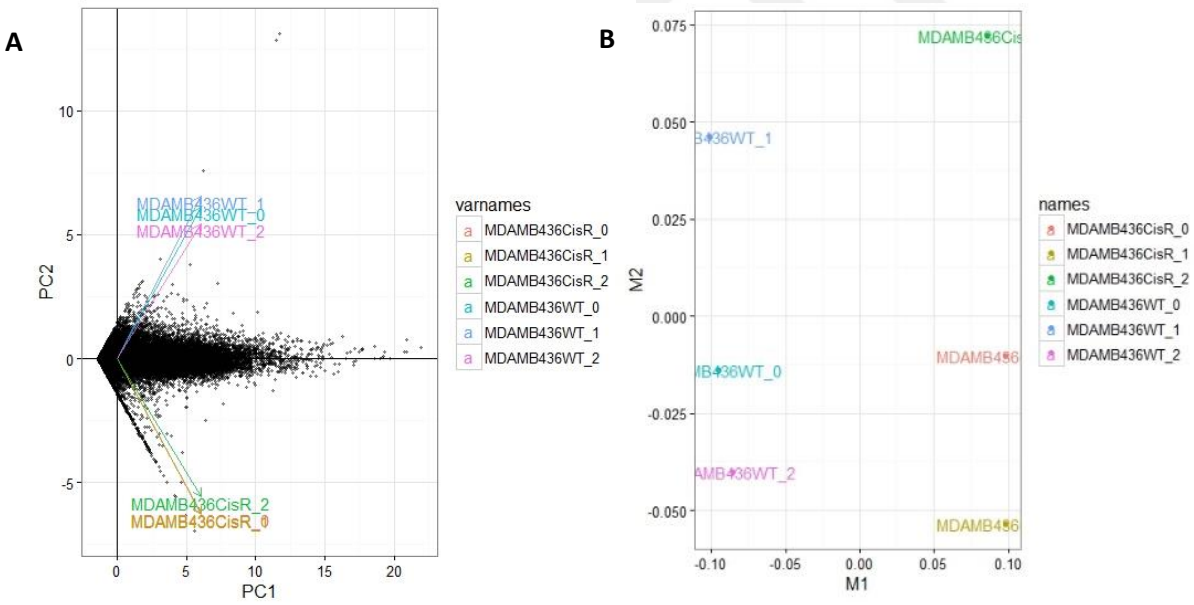

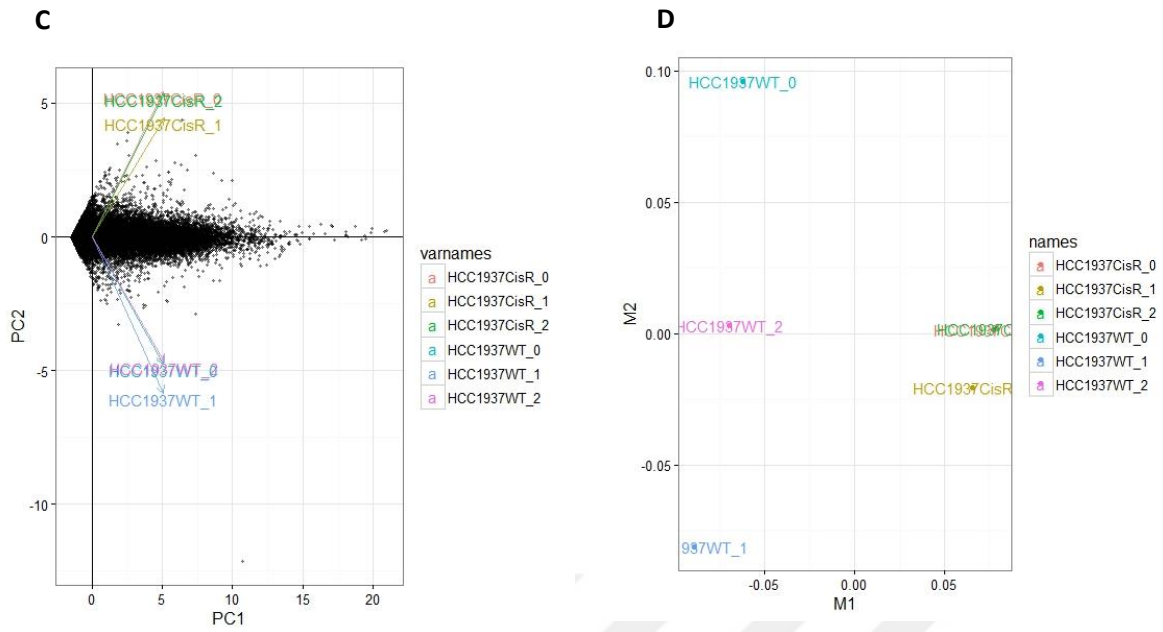

Figure 4.14. PCA and MDS plots showing the clustering of replicates and groups in MDA-MB-436 cells (**A** and **C**) and HCC1937 cells (**B** and **D**).

Finally, graphical representation of differentially expressed genes between conditions was made using volcano plots which provides both fold-change and stattistical significance information (Figure 4.15).

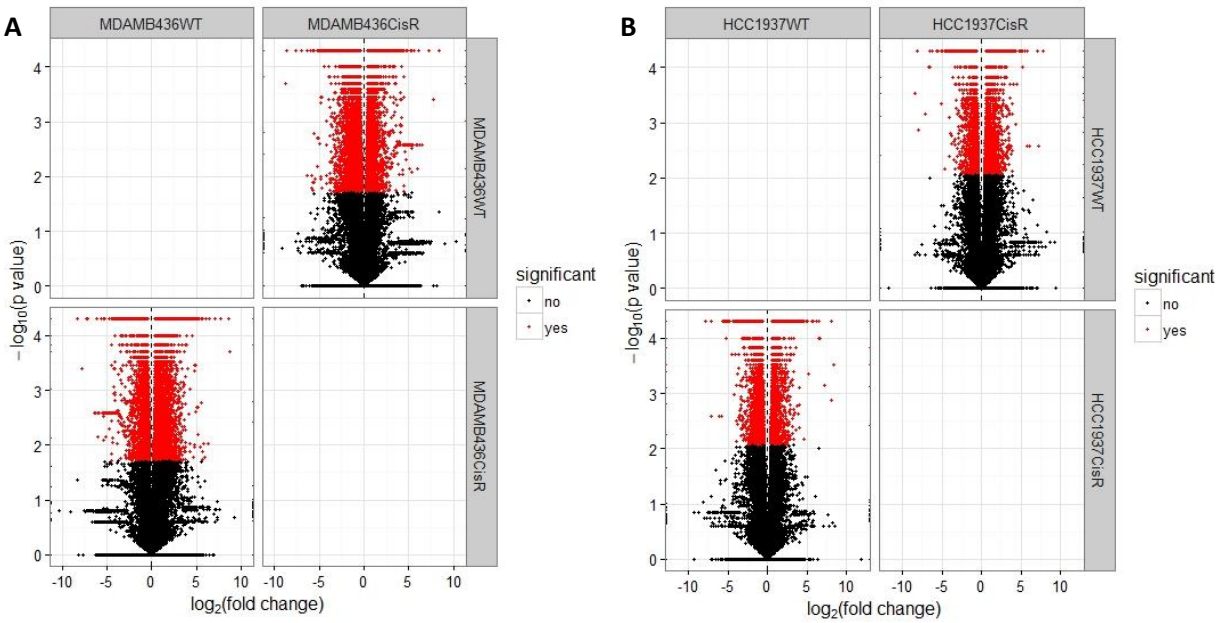

Figure 4.15. Volcano plots showing differentially expressed features between wild-type and resistant case in MDA-MB-436 (**A**) and HCC1937 (**B**). Red dots represents significantly (adjusted p-value less than 0.05) differentially expressed features.

After determining differentially expressed genes in each cell line model, we wanted to find out differentially expressed genes in Cisplatin resistance that are common for both cell lines. This strategy eliminates the cell line specific effect. According to the consensus results, 233 and 236 genes were significantly downregulated and upregulated in both models, respectively.

To determine the common genes that are highly deregulated in Cisplatin resistance, we applied $\log_2$fold-chance cut-off (greater and less than 1.5). Of these 469 genes that are significantly deregulated in both models, 25 genes passed this filter, of which 20 were downregulated and 5 were upregulated (Figure 4.16).

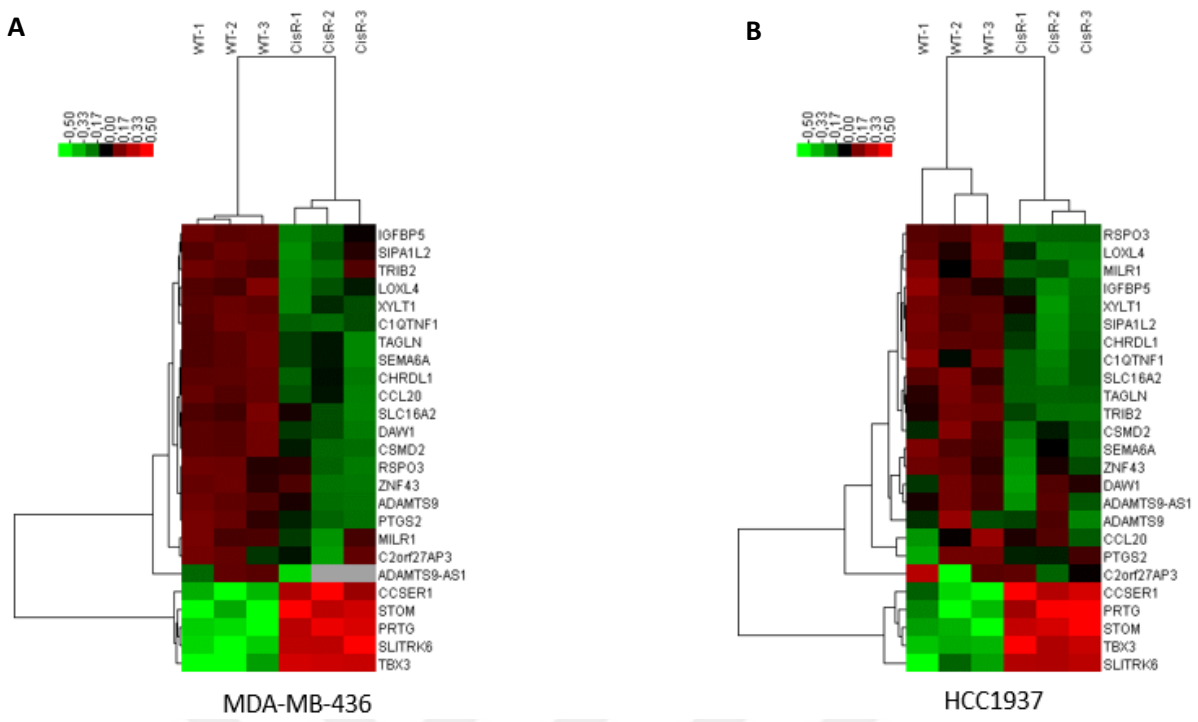

Figure 4.16. Representative heat-map graphics demonstrating highly deregulated 25 genes that passed the fold-change filter ($-1.5 \geq \log2FC \geq 1.5$) in MDA-MB-436 (**A**) and HCC1937 (**B**).

4.6. Identification of pathways commonly altered in both Cisplatin resistant models

Using these deregulated 469 gene list, IPA Core Analysis was done in order to find canonical pathways involved in Cisplatin resistance. Among these pathways, p53 signalling and ATM signalling, which are the regulators of DNA double strand break repair, were found to be positively regulated in Cisplatin resistance. On the other hand, integrin-linked kinase (ILK)

signalling, PI3K/AKT signalling and Protein Kinase A signalling pathways are the ones that negatively regulated (Figure 4.17).

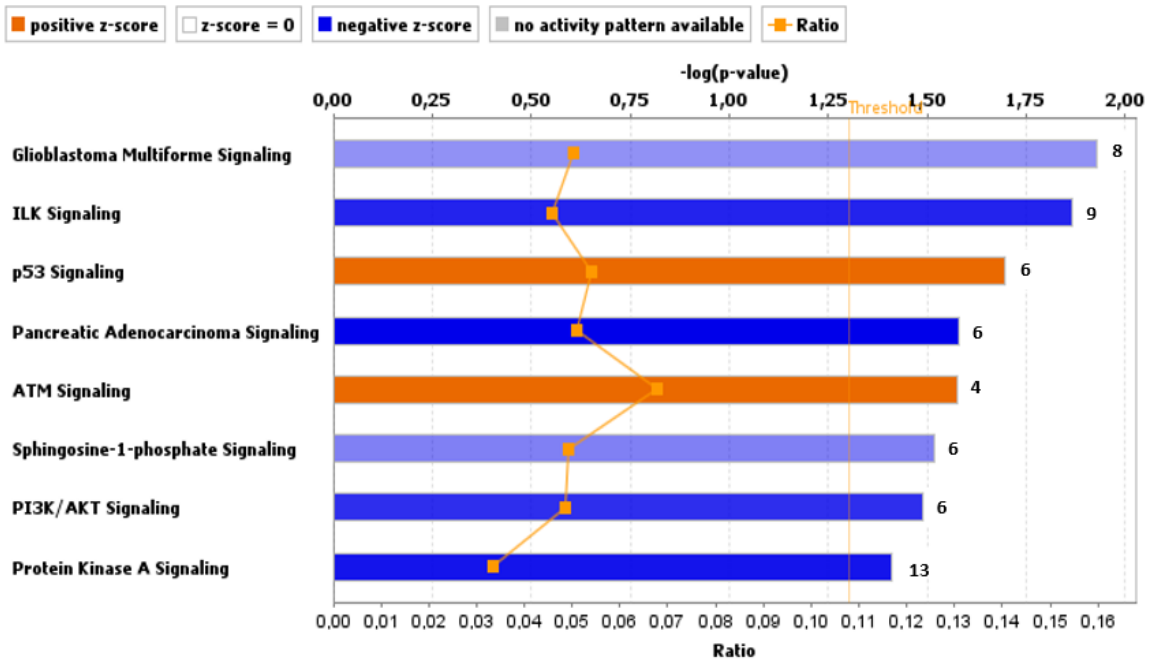

Figure 4.17. IPA Core Analysis graphic showing pathways deregulated in Cisplatin resistance. Pathways that are depicted in yellow have positive z-score (predicted to be activated in Cisplatin resistance) whereas blue depicted pathways have negative z-score (predicted to be inhibited in Cisplatin resistance). The numbers at the end of the bars show the number of overlapping genes between deregulated 469 genes and the genes that are involved in indicated IPA pathways.

Since Integrin-Linked Kinase (ILK) signalling, which is closely associated with EMT, is one of the most significantly deregulated pathways in Cisplatin resistance (Figure 4.17), we checked the expression status of EMT marker genes in HCC1937 model as this cell line is characterized as epithelial. Towards this end, we compared the expression level of 3 epithelial markers and 6 mesenchymal markers in both models using qRT-PCR (Figure 4.18). Results showed that epithelial markers ZO1 and KRT18 were significantly downregulated whereas some of

mesenchymal markers, specifically, FN and CDH2, were significantly upregulated after resistance. Of note, ZEB2 mesenchymal marker level is also increased in the resistant cells, but it is not statatistically significant. These results suggest that these cells may undergo partial EMT upon resistance development.

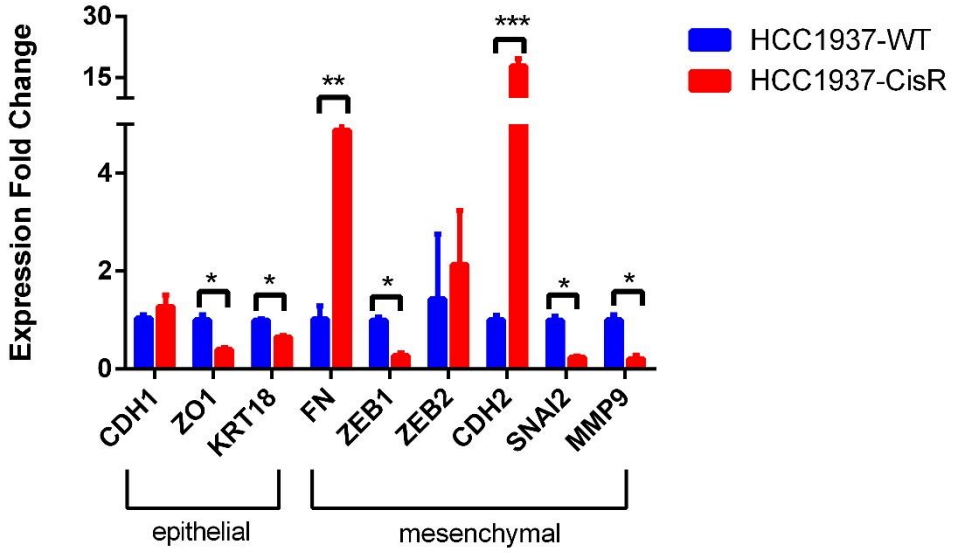

Figure 4.18. Expression status of EMT marker genes in HCC1937-WT and HCC1937-CisR cells. CDH1, ZO1, and KRT18 are epithelial markers. FN, ZEB1, ZEB2, CDH2, SNAI2, and MMP9 are mesenchymal markers. HPRT is used as housekeeping gene control (n=3).

IPA upstream regulator unravels the cascade of upstream transcriptional regulators that can control the observed expression change in a given data. It was found that *TP53* is the most significant upstream regulator of common deregulated genes (Figure 4.19), signifying the key role of p53 signalling in Cisplatin resistance.

Upstream Regulator	Exp Log Ratio	Molecule Type	Predicted Activation State	Activation z-score	p-value of overlap	Target molecules in d...	Mechanistic Network
TP53		transcription regulator		1,572	2,72E-09	↑ABHD4, ↑ADA, ↑... ...all 57	126 (18)
Cg		complex		0,947	1,58E-08	↑B2M, ↓BDNF, ↑B... ...all 24	124 (16)
TGFB1		growth factor		-0,017	4,53E-08	↓ARL4A, ↑B2M, ↓... ...all 60	156 (18)
beta-estradiol		chemical - endogenous ma...	Inhibited	-2,103	5,52E-08	↓ARL4A, ↓BDNF, ↑... ...all 63	145 (18)
forskolin		chemical toxicant		0,695	7,73E-08	↓BDNF, ↑BHLHE40, ·. ...all 33	109 (15)
Lh		complex	Inhibited	-2,145	9,26E-08	↓BDNF, ↑CAMK2G, ·. ...all 19	134 (19)
F2		peptidase		-1,820	1,27E-07	↓ADAMTS9, ↓AKR1B1 ...all 19	148 (14)
MYC		transcription regulator		-0,714	1,35E-07	↓BDNF, ↓BIRC2, ↓... ...all 43	148 (18)
IL1B		cytokine		-1,000	1,74E-07	↓AKR1B1, ↓ANTXR1 ...all 38	124 (12)
VEGFA		growth factor		-1,280	1,83E-07	↑CDKN1A, ↑CTSV, ↑... ...all 19	138 (17)
deferoxamine		chemical drug		0,881	2,30E-07	↓BDNF, ↑BHLHE40, ·. ...all 15	164 (21)
NFKBIA		transcription regulator		-0,402	2,47E-07	↓BIRC2, ↑BTG2, ↓... ...all 25	122 (16)
PDGF BB		complex		1,025	2,60E-07	↑ADD3, ↑BHLHE40, ·. ...all 21	145 (19)
methylprednisolone		chemical drug		-0,968	3,37E-07	↓ARL4A, ↓ATP5C1, ·. ...all 28	94 (11)
TNF		cytokine		-0,756	3,53E-07	↑ACADS, ↓AKR1B1, ·. ...all 58	131 (14)
Vegf		group		0,964	7,71E-07	↓C1QTNF1, ↑CDK2, ·. ...all 26	159 (17)
tretinoin		chemical - endogenous ma...	Activated	2,562	9,99E-07	↑ADA, ↑ADD3, ↑B... ...all 51	139 (18)
camptothecin		chemical drug		-0,079	1,09E-06	↓ARL4A, ↓BIRC2, ↑... ...all 29	119 (17)
SSRP1		other			1,44E-06	↑CDKN1A, ↑DUSP5, ·. ...all 7	76 (7)
FSH		complex	Inhibited	-2,663	1,62E-06	↓BDNF, ↑BTG2, ↑C... ...all 22	134 (18)
poly rI:rC-RNA		biologic drug		0,156	2,18E-06	↑B2M, ↓BIRC2, ↑C... ...all 23	109 (14)
CD24		other		1,000	2,28E-06	↑ADD3, ↑CDKN1A, ·. ...all 11	

Figure 4.19. IPA Upstream Regulator results showing the upstream regulators of 469 common genes regulating Cisplatin resistance in both cell lines. Regulators are sorted by p-value.

Gene Set Enrichment Analysis (GSEA) is a type of bioinformatics analysis that determines whether a set of genes has significant and concordant differences between two biological conditions. To test consistency of IPA findings, we performed GSEA analysis using the same 469 genes expressed differentially. Among KEGG pathways, P53 signalling pathway is the top significant pathway that is enriched in Cisplatin resistance (Normalized Enrichment Score (NES): -1.45, nominal p-value: 0.02) (Figure 4.20). Moreover, p53 signalling pathway from Hallmark gene signature sets was found to be enriched in resistant case (NES: -1.54, nominal p-value: 0.04). In conclusion, these results indicate a vital role of p53 signalling for Cisplatin resistance.

A

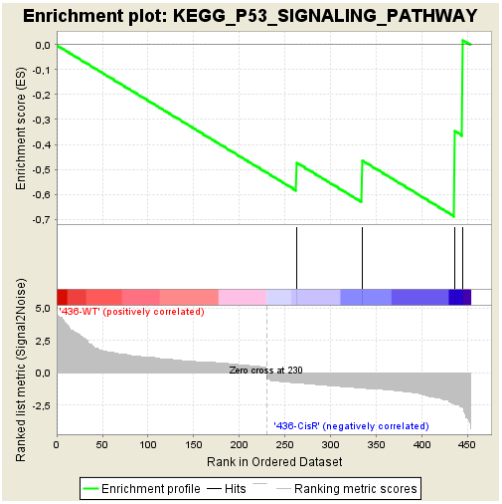

B

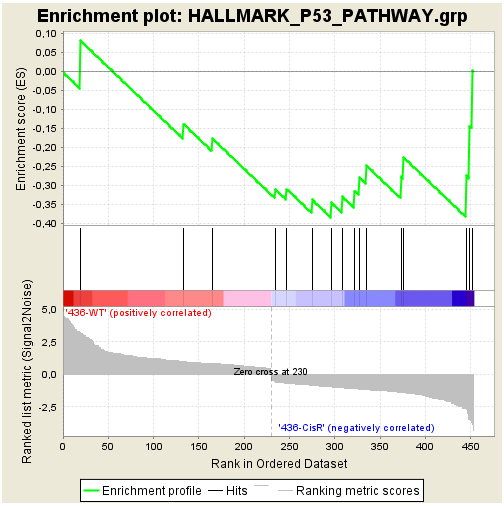

Figure 4.20. GSEA results for commonly deregulated 469 genes using gene signatures from KEGG pathway (NES: -1.45, nominal p-value: 0.02) (**A**) and Hallmark p53 signalling pathways (NES: -1.54, nominal p-value: 0.04) (**B**).

4.7. Construction of mRNA networks potentially involved in Cisplatin resistance

As IPA Core Analysis and IPA Upstream Regulator results as well as two GSEA results indicated that p53 signalling might be the main regulator of the resistance development. We constructed the p53 network regulating the genes that are differentially expressed in Cisplatin resistance using IPA (Figure 4.21).

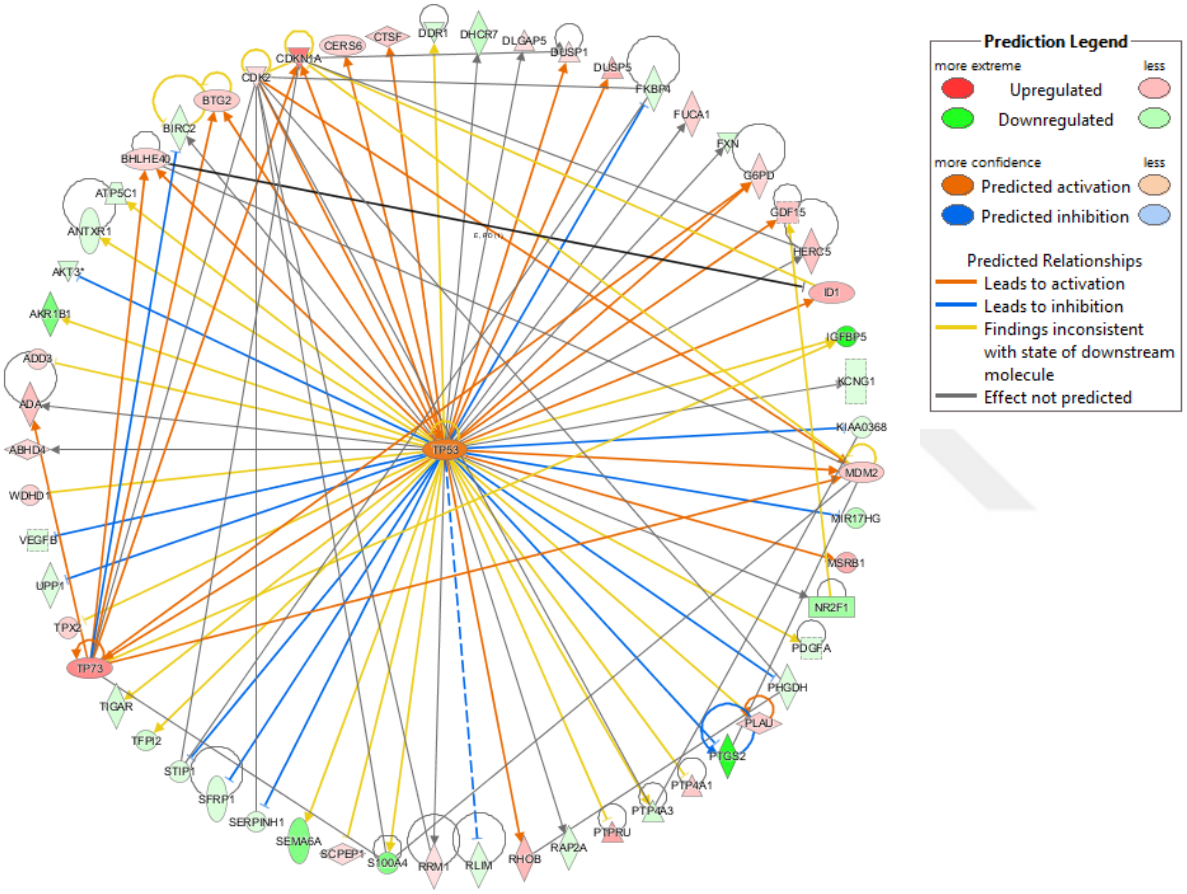

Figure 4.21: IPA Upstram Regulator showing p53 signalling pathway as network regulating genes involved in Cisplatin resistance. TP53 which is shown in orange was predicted to be activated. The genes that are green in colour are downregulated and the genes that are red in colour are upregulated in Cisplatin resistance. The interactions between genes that shown in blue lead to inhibition whereas the interactions in orange lead to activation. The yellow

interactions indicate inconsistent findings with respect to expression status of downstream molecule. The grey interactions show the type interactions that IPA can not predict.

After building the mRNA network regulating drug resistance, we integrated most differentially expressed miRNAs to this network in order to construct miRNA-mRNA network potentially involved in Cisplatin resistance. To this end, IPA microRNA target filter tool was used to find predicted targets of these miRNAs. At this point, target prediction was limited to differentially expressed mRNAs involved only in p53 upstream network. Furthermore, expression pairing between miRNAs and mRNAs was used to eliminate positively regulated targets of miRNAs. In other words, as miRNAs are the negative regulators of their target mRNAs, upregulated targets of a downregulated miRNA were removed. In conclusion, using paired small RNA-Seq and RNA-Seq data, we have identified p53 signalling centered miRNA-mRNA network potentially regulating Cisplatin resistance (Figure 4.22).

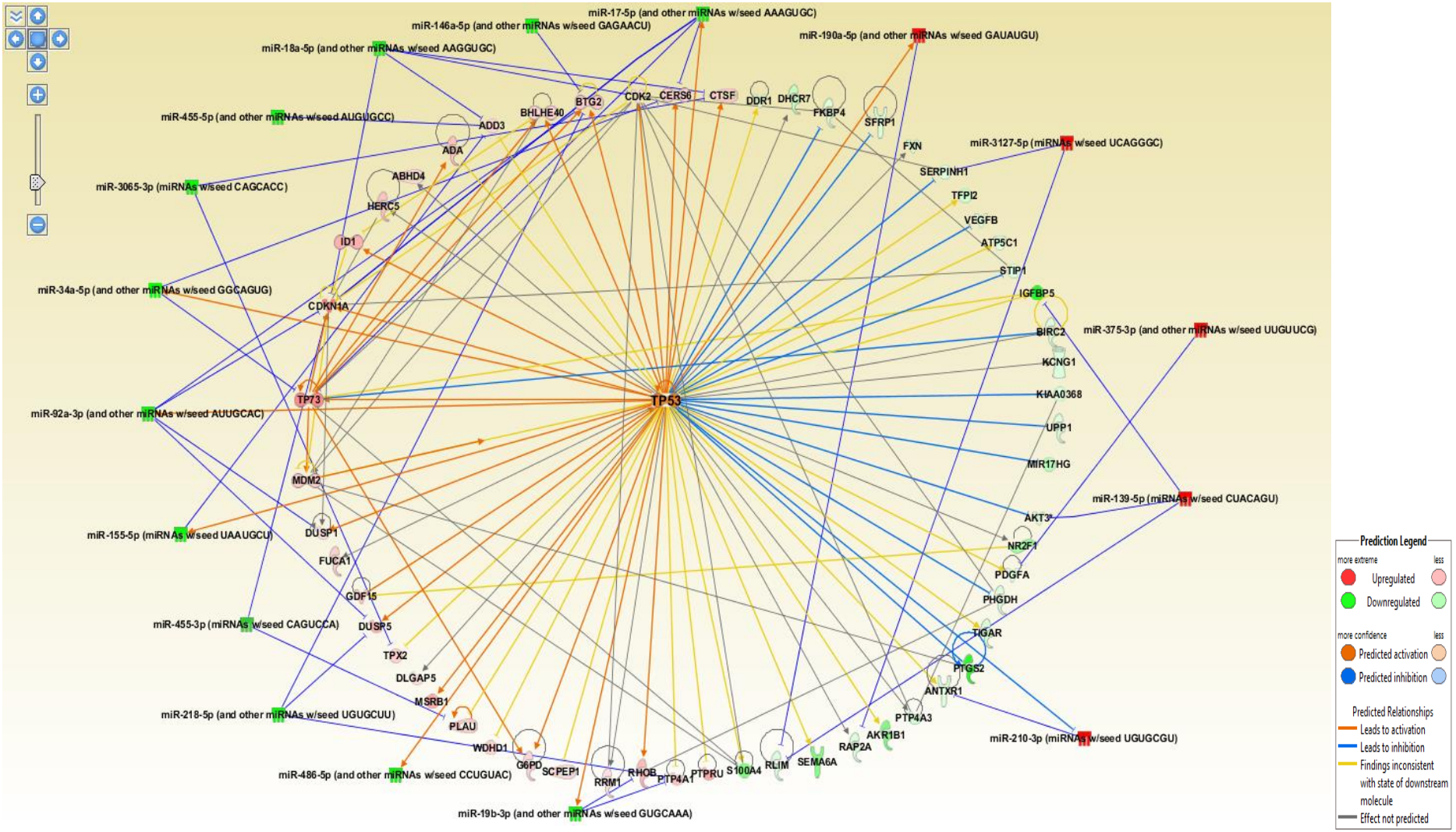
miR-17-5p (and other miRNAs w/seed AAAGUGC)
miR-146a-5p (and other miRNAs w/seed GAGAACU)
miR-190a-5p (and other miRNAs w/seed GAUAUGU)
miR-18a-5p (and other miRNAs w/seed AAGGUGC)
miR-455-5p (and other miRNAs w/seed AUGUGCC)
miR-3127-5p (miRNAs w/seed UCAGGGC)
miR-3065-3p (miRNAs w/seed CAGCACC)
miR-34a-5p (and other miRNAs w/seed GGCAGUG)
miR-375-3p (and other miRNAs w/seed UUGUUCG)
miR-92a-3p (and other miRNAs w/seed AUUGCAC)
miR-139-5p (miRNAs w/seed CUACAGU)
miR-155-5p (miRNAs w/seed UAAUGCU)
miR-455-3p (miRNAs w/seed CAGUCCA)
miR-218-5p (and other miRNAs w/seed UGUGCUU)
miR-210-3p (miRNAs w/seed UGUGCGU)
miR-486-5p (and other miRNAs w/seed CCUGUAC)
miR-19b-3p (and other miRNAs w/seed GUGCAAA)
TP53
TP73
MDM2
CDKN1A
BTG2
CDK2
CERS6
CTSF
DDR1
DHCR7
FKBP4
SFRP1
BHLHE40
ADD3
ADA
ABHD4
HERC5
ID1
FXN
SERPINH1
TFPI2
VEGFB
ATP5C1
STIP1
IGFBP5
BIRC2
KCNG1
KIAA0368
UPP1
MIR17HG
AKT3
NR2F1
PDGFA
PHGDH
TIGAR
PTGS2
ANTXR1
PTP4A3
AKR1B1
RAP2A
SEMA6A
RLIM
S100A4
PTPRU
PTP4A1
RRM1
RHOB
SCPEP1
G6PD
WDHD1
PLAU
MSRB1
DLGAP5
TPX2
DUSP5
GDF15
FUCA1
DUSP1
Prediction Legend
more extreme
less
Upregulated
Downregulated
more confidence
less
Predicted activation
Predicted inhibition
Predicted Relationships
Leads to activation
Leads to inhibition
Findings inconsistent with state of downstream molecule
Effect not predicted

Figure 4.22. miRNA-mRNA network regulating Cisplatin resistance. TP53 which is shown in orange was predicted to be activated. The genes that are green in colour are downregulated and the genes that are red in colour are upregulated in Cisplatin resistance. The interactions between genes that shown in blue lead to inhibition whereas the interactions in orange lead to activation. The yellow interactions indicate inconsistent findings with respect to expression status of downstream molecule. The grey interactions show the type interactions that IPA can not predict.

4.7.1. miRNA-transcription factor co-regulation in Cisplatin resistance

Transcriptional and post-transcriptional regulators are important in modulation of gene expression and various signalling pathways. miRNAs regulate their target in a network manner and transcription factors are involved in this network by acting different roles; interacting with miRNA and/or predicted target of the miRNA. Depending on type of these interactions, there are two main motifs of miRNA-transcription factor co-regulation: coherent feedforward loops and incoherent feedforward loops.

4.7.1.1. Coherent feedforward loops

In this type of co-regulation motif, predicted targets of miRNAs are regulated in the same direction by miRNA and transcription factor. In other words, the target is co-repressed and this repression is depended on reinforcement between miRNA and transcription factor. When we generate sub-group motifs from miRNA-mRNA network, we see examples of this co-regulation. For example, miR-34c-5p targets and inhibits transcriptional factor p53 which positively regulates miR-34c-5p. As predicted targets, *CTSF* and *TP73*, positively regulated by transcription factor, the entire system works to reduce the level of targets (Figure 4.23).

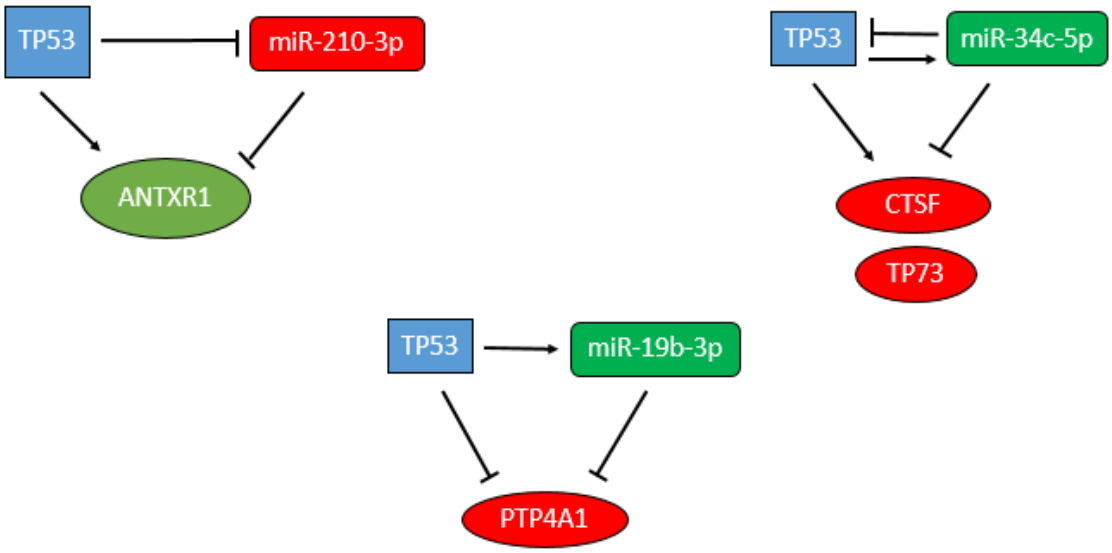

Figure 4.23. Graphical representation of motifs that show coherent feedforward loop trait. Transcription factor is shown in blue, downregulated features are shown in green and upregulated features are shown in red colour according to the log2FC values from our small RNA-Seq and RNA-Seq data.

4.7.1.2. Incoherent feedforward loops

Incoherent feedforward loops are one of the most common motifs in which miRNA and transcription factor play opposing roles. It is, therefore, important type of regulation that allows stability of the system. In our system, for instance, on the one hand, miR-19-3p tries to inhibit RHOB levels. On the other hand, p53 activates both miR-19-3p and its target RHOB, suggesting an incoherent type of interaction tries to balance target expression level (Figure 4.24).

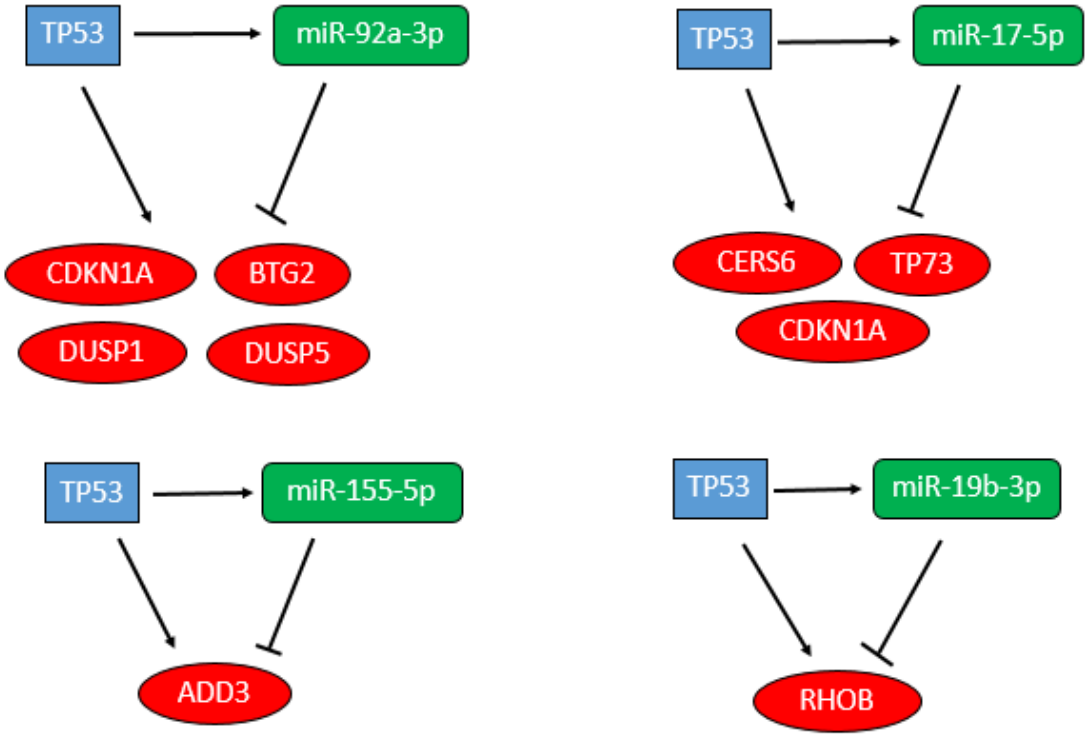

Figure 4.24. Graphical representation of motifs that show incoherent feedforward loop trait. Transcription factor is shown in blue, downregulated features are shown in green and upregulated features are shown in red colour according to the log2FC values from our small RNA-Seq and RNA-Seq data.

4.8. miR-455-3p and miR-455-5p and their predicted target networks in Cisplatin resistance

We have shown that miR-455-3p and miR-455-5p sensitized resistant cells to Cisplatin. Therefore, we also constructed the sub-networks including the targets of these miRNAs (Figure 4.25). Accordingly, miR-455-5p is involved in a relatively small motif where it targets *ADD3* which is also negatively regulated by TP53. miR-455-3p, on the other hand, is the regulator of much more complex motif. Specifically, miR-455-3p is predicted to be targeting *PLAU* and *CDKN1A*. *PLAU* is also targeted by p53 transcription factor. *CDKN1A* has different types of

interactions with TP73, CDK2, ID1 and MDM2. This model may shed light on the mechanism of Cisplatin sensitization effect of these miRNAs with respect to downstream gene regulators contributing to the resistance process.

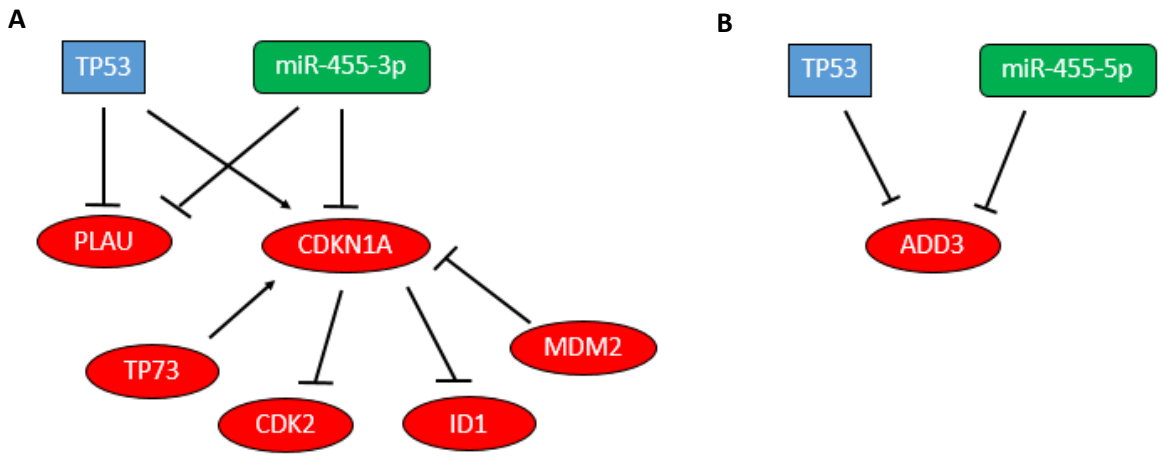

Figure 4.25. Motifs modified from p53 signalling based miRNA-mRNA network showing predicted targets of miR-455-3p (**A**) and miR-455-5p (**B**). Transcription factor is shown in blue, downregulated features are shown in green and upregulated features are shown in red colour according to the log2FC values from our small RNA-Seq and RNA-Seq data.

Chapter 5

Discussion

This thesis has shown different miRNA-mRNA regulatory networks that might provide a rationale explanation for Cisplatin resistance at the molecular level. For the first time, this study has reported miR-455 effect on Cisplatin resistance in breast cancer. Developing acquired chemotherapy resistant cell line model and using next generation sequencing technology, we have unravelled the underlying molecular changes of Cisplatin resistance. Moreover, with the use of IPA which uses omics data from a variety of experimental platforms, we analyzed, combined and modelled miRNA-mRNA interactions and identified several network motifs potentially regulating Cisplatin resistance for the first time.

5.1. Small RNA-Seq and miRNA candidates in Cisplatin resistance

RNA-Seq outperforms array-based technologies, such as microarrays, in terms of detection of novel transcripts, increased sensitivity and specifity and detection of rare and low-expressed transcripts due to high sequencing depth [52] [53]. Thus, we preferred using RNA-Seq technology to better achieve our aim of the study. As mentioned earlier, small RNA-Seq was performed to elucidate miRNAs controlling Cisplatin resistance in *BRCA1*-mutated TNBC cell lines. In total 32 miRNAs were found to be dsyregulated commonly in both cell lines. It is important to investigate the consistency of our data with previous literature findings with respect to miRNA alterations in response to chemotherapy drugs. In this regard, the most downregulated miRNA, miR-34c, has been shown to enhance Cisplatin response in endometrial cancer, suggesting tumor suppressor role of the miRNA [54]. Likewise, low expression of miR-146a is found to be associated with poor patient survival in consistent with the our findings. In

the same study, researchers also demonstrated that miR-146a promoter was targeted by BRCA1. Activated miR-146a, in turn, targets EGFR and inhibits it resulting in decreased proliferation and clonogenic growth [55]. Moreover, miR-375 whose forced expression is found to reverse Tamoxifen resistance by our group [33] acted as an onco-miR in paclitaxel resistant cervical cancer [56] in line with upregulation in this study. These lines of evidence support our findings and prove the quality and consistency of our data.

5.2. RNA-Seq and integrating miRNA-mRNA network

5.2.1. Potential role of p53 pathway in Cisplatin resistance

5.2.1.1 DNA damage recognition, p53 activation, and apoptosis

p53, which is the protein product of *TP53* gene, is tumor-suppressor protein that has pleiotropic effects on apoptosis, genomic stability, DNA damage, and cell cycle [57]. For example, in order for p53 to induce Cisplatin-mediated apoptosis, activation and stability of wild-type p53 is necessary. To activate the p53 tumor suppressor as a consequence of Cisplatin-directed DNA damage, particular upstream signalling events are required. These include activity of important kinases, namely, ATM (ataxia telangiectasia mutated protein) and ATR (ATM- and Rad3-related protein), that are involved in checkpoint activation [58]. Cisplatin exerts its role mostly through ATR pathway [59]. ATR phosphorylates p53 at serine-15, resulting in activation of the p53 protein [60]. Besides, downstream target of the ATR, CHK1, phosphorylates p53 at serine-20 [61], intensifying p53 activation. Downstream target of ATM, CHK2, is also activated by Cisplatin-mediated response, but this effect is not dependent on ATM signalling [58].

$p21^{Waf1/Cip1}$, *GADD45A*, *BAX* genes that are related to cell cycle arrest, DNA repair, and apoptosis, respectively, are transactivated by p53 in response to Cisplatin treatment [62] [63] [64] [65]. Of note, MDM2, which is upregulated in our resistant network, is also transactivated by p53 protein and it is a negative feedback regulator of p53 [66] . Gadd45a protein has been

shown to prevent cisplatin-mediated toxicity by improving Nucleotide Excision Repair (NER) activity [62] [65]. Nevertheless, apoptosis is inevitable when DNA damage is beyond the repair capacity of the cell. In this regard, Bax causes activation of the caspase 9–caspase 3 pathway which leads to apoptosis [67] [68]. In detail, the ratio between the pro-apoptotic Bax and the anti-apoptotic Bcl-2 is the main modulator when apoptosis decision made by the cell. At this point, Cisplatin is capable of inducing Bax or cleavage of Bcl-2, both of which decreases Bax:Bcl-2 ratio and therefore leads to apoptosis [69]. Additionally, apoptosis can be triggered by caspase 8–caspase 3 pathway that requires activation of Fas/FasL by p53 [70] .

5.2.1.2. p53-mediated DNA damage repair increase and dysfunction of mutated p53

The effect of Cisplatin with respect to cytotoxicity is mostly ascribed to formation of intrastrand crosslinks in DNA [71]. In detail, 1,2-intrastrand ApG and GpG crosslinks are the main type of DNA adducts which trigger cytotoxicity [72]. Tolerance to Cisplatin adducts, which is one of the mechanism of action for drug insensitization, is closely related to Cisplatin resistance and there is a correlation between DNA damage tolerance and the extent of the drug resistance [73] [74].

Increase in DNA damage repair is another prime factor contributing to Cisplatin resistance to attenuate apoptosis. NER is of the considerable impact on Cisplatin adduct removal as shown by hypersensitivity to Cisplatin in NER malfunctioning cells [75]. Cisplatin resistance caused by NER is generally ascribed to elevated levels of ERCC1 or ERCC1/XPF complexes as well as XPA gene overexpression [75] [76]. Consistently, in our RNA-Seq data, we observed a significant increase in both ERCC1 (log2FC of 0.79) and XPA (log2FC of 0.82) levels in MDA-MB-436-CisR cells. However, both genes were downregulated in HCC1937-CisR cells. Another repair mechanism that contributes to DNA damage repair is MMR which is responsible for recognizing DNA damage and repairing DNA mismatch lesions, but not Cisplatin adducts [77]. Repair of DNA takes place before DNA replication to make sure that genome stability is

preserved. Nonetheless, resistant cells can behave against this genome integrity protection by performing post-replication repair [75]. This replicative bypass provides high tolerance to Cisplatin-induced DNA adducts. Consistent with this, Cisplatin-resistant tumor cells tend to have downregulated levels of MMR genes and thus reduced apoptosis [78] [79]. However, there are cases in which this bypass occurs independently from MMR. In such cases, it has been shown that loss of p53 is responsible for the Cisplatin resistance [80] [81].

There are numerous reports on p53 signalling involvement in Cisplatin resistance. One of the first reports indicated that depletion of p53 protein resulted in 8-fold increase to Cisplatin resistance in ovarian cancer [82] . Additionally, several other *in vitro* and *in vivo* results have showed that *p53* gene mutations and subsequent abnormal p53 signalling can initiate and sustain Cisplatin resistance [83] [84] [85]. Recently, we have also shown that miR-644a directly targets CTBP1, resulting in increased wild type or mutant p53. We then observed that mutant p53 mediated apoptosis through Noxa whereas wild type p53 provoked G1-arrest by inducing $p21^{Waf1/Cip1}$ [86].

Mutations in exons 4-9 of p53 are commonly observed in cancer and are associated with p53-related pathological conditions [87]. More specifically, presence of these exon specific mutations leads to disruption of the ability of p53 to bind to DNA and activate signalling cascade, in other words, causing prevention of apoptotic property of *p53*. HCC1937 cells have C- > T mutation in exon 8 of TP53 [88] whereas MDA-MB-436 cells have a frameship type of mutation in exon 6 [89]. Therefore it is very likely to bypass cell death program and develop resistance towards drugs that create DNA damage, supporting our findings.

In addition, cancer cells are most sensitive to Cisplatin in G1 phase of the cell cyle and the fact that mutant p53 negates cell cycle arrest in G1 suggests that resistance development through p53 inactivation may be dependent on cell cycle checkpoints [90]. When cell cycle proteins come into play, $p21^{Waf1/Cip1}$ is one of the primary regulators that should be mentioned. It has

been shown that disrupted p21 sensitizes cells to Cisplatin in p53 dependent manner [91]. This observation could be related to G2/M arrest due to downregulation of p21 and subsequent premature entry to mitosis that leads to cell death. Consistently, we also found this gene to be highly upregulated in Cisplatin resistance. Moreover, *HER-2/neu* overexpression was found to confer Cisplatin resistance [92], and we observed that it is upregulated in resistance in RNA-Seq data. This overexpression improves Akt activity which is responsible for cytoplasmic localization of p21 [93]. The resulting decrease in nuclear p21 levels might be the reason for Cisplatin-mediated proliferative effects. Overall, these studies have concluded that p53 mutations may lead to failure in G1/S checkpoint control and therefore inhibiting the ability of p53 to induce apoptosis in response to DNA damage. In addition, p53 dependent p21 overexpression or PI3-K/Akt pathway-mediated induction of $p21^{Waf1/Cip1}$ in *HER-2/neu* overexpressing cells may exacerbate the Cisplatin resistance.

5.2.2. Motifs in p53-mediated Cisplatin network

5.2.2.1 Coherent Feedforward Loops

One of the upregulated miRNAs, miR-210-3p, and two of the downregulated miRNAs, miR-34c-5p and miR-19b-3p, are involved in this type of network motifs. Importantly, when considering the expression status of particular members of this sub-network, only miR-34c-5p fits with RNA-Seq results; miR-34c-5p targets and inhibits both transcription factor (TP53) and mRNAs (TP73 and CTSF) and as TP53 activates mRNAs, system works as expression enhancer of mRNA targets. Cathepsin F, *CTSF*, is a protein coding gene that is involved in lysosomal proteolytic system activity. It was found that CTSF is one of the components of degradome-related gene signatures that favours metastatic stem-like profile in acquired metformin resistance in MCF-7 cells [94]. More importantly, CTSF was found to be downregulated in

mouse embryonic fibroblasts (MEFs) that engineered to have p53 loss [95]. On the other hand, tumor protein P73 is an important regulator of apoptotic response to DNA damage. In a study, DNA repair associated molecules ATM, CHK1, TP73, p53, and ERCC1 were found to be upregulated IL-6 knocked down xenografts generated by human NSCLC cells that shown to be Cisplatin resistant as compared to IL-6 wild-type cells [96], suppoting our findings.

5.2.2.2 Incoherent Feedforward Loops

For resistance development and stability *via* incoherent feeforward loops, the involvement of miR-17/92 cluster might be important. We realized that except miR-155-5p, all incoherent feedforward loop motifs are components of miR-17/92 cluster. Specifically, miR-92a-3p, miR-17-5p and miR-19b-3p regulates mRNA target levels together with trascription factor p53 and are also predicted to be regulated by p53. As mentioned earlier, these type of motifs are characterized by balancing the target levels and stabilize the system. For example, p53 positively regulates both RHOB and miR-19b-3p and the latter induces inhibition of RHOB. In this scenario, RHOB expression is negatively influenced by microRNA and positively influenced by transcription factor, resulting in upregulation of the targets. Indeed, there might be other factors changing the levels of the target Mrna, but here p53 effect over miRNA seems more impactful. *RHOB*, Ras Homolog Family Member B, encodes a small GTPase that modulate actin cytoskeleton. It has been shown that downregulation of RHOB resulted in resistance to Cisplatin in human laryngeal carcinoma cells, but this effect was not observed in other type cancer cell lines, suggesting cancer specific effect. Upon DNA damage, RHOB is thought to be take part in apoptosis pathway as a downstream partner of ATM or p53 signalling, suggesting its potential role in Cisplatin resistance.

5.3 miR-17/92 cluster and chemotheraphy resistance

Polycistronic miR-17/92 cluster which is also known as 'oncomiR-1' is of great importance in normal development [97] as well as pathologic conditions related to aberrant proliferation, apoptosis and cell cyle regulation [98] [99] [100]. As the name suggests, it is the first identified oncogenic miRNA [101]. *C13orf25* or *MIR17HG* was found to be the host gene for the miR-17/92 cluster which consists of 6 miRNAs: miR-17, miR-18a, miR-19a, miR-20a, miR-19b-1 and miR-92a-1. This cluster has two paralogue clusters in the genome, namely, miR-106b/25 and the miR-106a/363. The miR-106b/25 cluster is composed of miR-106b, miR-93 and miR-25 whereas miR-106a, miR-18b, miR-20b, miR-19b-2, miR-92a-2 and miR-363 form the miR-106a/363 cluster [102]. All together these clusters create 4 crucial miRNA families in which each family members share the same seed sequence. These families are the miR-17 family, the miR-18 family, the miR-19 family and the miR-92 family. Importantly, it has been shown that, all but miR-106a/363 cluster, is highly expressed in various tissues [103] [104].

The role of miR-17/92 cluster in normal versus pathological conditions can demonstrate oncogenic and/or tumor suppressive features. In a study using deep sequencing for TNBC samples, miR-17/92 levels were shown to be increased in tumor versus normal tissue [105]. Another study revealed that microRNA17/20 has higher expression in non-invasive breast cancer cell lines as compared to highly invasive cells and controls breast cancer migration and invasion, suggesting a tumor suppressor role for the miRNAs [100]. In the context of chemo-resistance, it was found that miR-17/92 cluster confers Cisplatin resistance through modulation of AKT and ERK1/2 signalling pathways in prostate cancer cells [106]. In contrast, our work has found that expression level miR-17/92 cluster members reduced in Cisplatin resistance. This again suggests cancer context-dependent functions of miRNAs.

5.4 miR-455 and chemotherapy sensitivity/resistance

miR-455 family consists of two members, miR-455-3p and miR-455-5p. According to the recent classification system in TargetScan database miR-455-3p is divided further into 2 sub-clasesses which are miR-455-3p.1 and miR-455-3p.2 [107]. Sequence match analysis showed that miR-455-3p is represented in TargetScan as miR-455-3p.1. These members have different seed sequence and therefore can target completely different mRNA profile. miR-455 has been reported to act as a tumor suppressor miRNA in different spectra of cancers [108] [109] [110], strengthening the findings reported here. Thus far, no study reported the role of miR-455 in breast cancer. Hence, this study is the first one linking miR-455 with breast cancer.

Chemotherapy response/resistance and miR-455 have been studied in different context and cancers. For instance, miR-455-3p is one of the upregulated miRNAs involved in acquired temozolomide resistance in glioblastoma multiforme (GBM) [111]. Consistently, IPA Core Analysis found that GBM signalling is the most deregulated pathway. Additionally, miR-455-3p was found to be downregulated in chemoresistant colon cancer. In an another study examining the short-term (24h) and long-term (72h) Cisplatin exposure in esophageal cancer, miR-455-3p was shown to be downregulated in dose-dependent manner [112], which is consistent with the acquired resistant model described here. In conclusion, depending on the host tissue, cancer type and chemotherapy choice, miR-455 expression level can vary.

Chapter 6

Conclusions and Future Perspectives

In this this study, we found coherent and incoherent feedforward loops that have high potential to modulate Cisplatin resistance within p53 signalling pathway in BRCA1-mutated TNBCs. So far, the study relies mostly on bioinformatic analyses that revealed core targets within network motifs that might be a solid basis for Cisplatin resistance. It is therefore important to provide further experimental validation for the involvement of these network motifs in resistance and reversing the resistance. To do this, one might first show miRNAs in the motifs target the predicted mRNAs and with the interaction with p53, system works to provide the resistance. In order to revert the resistance, Clustered Regularly Interspaced Short Palindromic Repeats (CRISPR) interference could be used to knock-out mRNAs in the presence of Cisplatin. Therapeutically, CGM097 can be used to disrupt p53 signalling dictating Cisplatin resistance and thus causing sensitization as this drug is a selective inhibitor of MDM2/TP53 which are the key upregulated regulators of the resistant network.

Although we showed the miR-455-3p and miR-455-5p upregulation can sensitize cells to Cisplatin, it is needed to decipher molecular mechanims responsible for the resistance. At this point, motifs in p53 signalling pathway can help us to find targets of these miRNAs to validate. For example, it is very likely to happen a CDKN1A centered resistance mechanism in miR-455-3p containing motif as it is an important regulator of cell cycle and DNA damage response in response to Cisplatin.

Bibliography

1. Hutchinson, L., *Breast cancer: challenges, controversies, breakthroughs.* Nat Rev Clin Oncol, 2010. **7**(12): p. 669-70.
2. Jemal, A., et al., *Cancer statistics, 2010.* CA Cancer J Clin, 2010. **60**(5): p. 277-300.
3. Sorlie, T., et al., *Repeated observation of breast tumor subtypes in independent gene expression data sets.* Proc Natl Acad Sci U S A, 2003. **100**(14): p. 8418-23.
4. de Ronde, J., L. Wessels, and J. Wesseling, *Molecular subtyping of breast cancer: ready to use?* Lancet Oncol, 2010. **11**(4): p. 306-7.
5. Morgan, D.A., N.A. Refalo, and K.L. Cheung, *Strength of ER-positivity in relation to survival in ER-positive breast cancer treated by adjuvant tamoxifen as sole systemic therapy.* Breast, 2011. **20**(3): p. 215-9.
6. Gajria, D. and S. Chandarlapaty, *HER2-amplified breast cancer: mechanisms of trastuzumab resistance and novel targeted therapies.* Expert Rev Anticancer Ther, 2011. **11**(2): p. 263-75.
7. Sorlie, T., et al., *Gene expression patterns of breast carcinomas distinguish tumor subclasses with clinical implications.* Proc Natl Acad Sci U S A, 2001. **98**(19): p. 10869-74.
8. Liedtke, C., et al., *Response to neoadjuvant therapy and long-term survival in patients with triple-negative breast cancer.* J Clin Oncol, 2008. **26**(8): p. 1275-81.
9. Rastogi, P., et al., *Preoperative chemotherapy: updates of National Surgical Adjuvant Breast and Bowel Project Protocols B-18 and B-27.* J Clin Oncol, 2008. **26**(5): p. 778-85.
10. Hall, J.M., et al., *Linkage of early-onset familial breast cancer to chromosome 17q21.* Science, 1990. **250**(4988): p. 1684-9.
11. Futreal, P.A., et al., *BRCA1 mutations in primary breast and ovarian carcinomas.* Science, 1994. **266**(5182): p. 120-2.
12. Miki, Y., et al., *A strong candidate for the breast and ovarian cancer susceptibility gene BRCA1.* Science, 1994. **266**(5182): p. 66-71.
13. Manke, I.A., et al., *BRCT repeats as phosphopeptide-binding modules involved in protein targeting.* Science, 2003. **302**(5645): p. 636-9.
14. Yu, X., et al., *The BRCT domain is a phospho-protein binding domain.* Science, 2003. **302**(5645): p. 639-42.
15. Monteiro, A.N., A. August, and H. Hanafusa, *Evidence for a transcriptional activation function of BRCA1 C-terminal region.* Proc Natl Acad Sci U S A, 1996. **93**(24): p. 13595-9.
16. Williams, R.S. and J.N. Glover, *Structural consequences of a cancer-causing BRCA1-BRCT missense mutation.* J Biol Chem, 2003. **278**(4): p. 2630-5.
17. Nathanson, K.L., R. Wooster, and B.L. Weber, *Breast cancer genetics: what we know and what we need.* Nat Med, 2001. **7**(5): p. 552-6.
18. Foulkes, W.D., et al., *Germline BRCA1 mutations and a basal epithelial phenotype in breast cancer.* J Natl Cancer Inst, 2003. **95**(19): p. 1482-5.
19. Manie, E., et al., *High frequency of TP53 mutation in BRCA1 and sporadic basal-like carcinomas but not in BRCA1 luminal breast tumors.* Cancer Res, 2009. **69**(2): p. 663-71.
20. Dai, X., et al., *Breast cancer intrinsic subtype classification, clinical use and future trends.* Am J Cancer Res, 2015. **5**(10): p. 2929-43.
21. Wang, D. and S.J. Lippard, *Cellular processing of platinum anticancer drugs.* Nat Rev Drug Discov, 2005. **4**(4): p. 307-20.
22. Ashworth, A., *A synthetic lethal therapeutic approach: poly(ADP) ribose polymerase inhibitors for the treatment of cancers deficient in DNA double-strand break repair.* J Clin Oncol, 2008. **26**(22): p. 3785-90.
23. Tassone, P., et al., *BRCA1 expression modulates chemosensitivity of BRCA1-defective HCC1937 human breast cancer cells.* Br J Cancer, 2003. **88**(8): p. 1285-91.

24. Byrski, T., et al., *Response to neoadjuvant therapy with cisplatin in BRCA1-positive breast cancer patients.* Breast Cancer Res Treat, 2009. **115**(2): p. 359-63.
25. Byrski, T., et al., *Pathologic complete response rates in young women with BRCA1-positive breast cancers after neoadjuvant chemotherapy.* J Clin Oncol, 2010. **28**(3): p. 375-9.
26. Ambros, V., *The functions of animal microRNAs.* Nature, 2004. **431**(7006): p. 350-5.
27. Bartel, D.P., *MicroRNAs: genomics, biogenesis, mechanism, and function.* Cell, 2004. **116**(2): p. 281-97.
28. Winter, J., et al., *Many roads to maturity: microRNA biogenesis pathways and their regulation.* Nat Cell Biol, 2009. **11**(3): p. 228-34.
29. Kozomara, A. and S. Griffiths-Jones, *miRBase: integrating microRNA annotation and deep-sequencing data.* Nucleic Acids Res, 2011. **39**(Database issue): p. D152-7.
30. Tam, S., et al., *Robust global microRNA expression profiling using next-generation sequencing technologies.* Lab Invest, 2014. **94**(3): p. 350-8.
31. Sayed, D. and M. Abdellatif, *MicroRNAs in development and disease.* Physiol Rev, 2011. **91**(3): p. 827-87.
32. Raza, U., J.D. Zhang, and O. Sahin, *MicroRNAs: master regulators of drug resistance, stemness, and metastasis.* J Mol Med (Berl), 2014. **92**(4): p. 321-36.
33. Ward, A., et al., *Re-expression of microRNA-375 reverses both tamoxifen resistance and accompanying EMT-like properties in breast cancer.* Oncogene, 2013. **32**(9): p. 1173-82.
34. Jurmeister, S., et al., *MicroRNA-200c represses migration and invasion of breast cancer cells by targeting actin-regulatory proteins FHOD1 and PPM1F.* Mol Cell Biol, 2012. **32**(3): p. 633-51.
35. Uhlmann, S., et al., *miR-200bc/429 cluster targets PLCgamma1 and differentially regulates proliferation and EGF-driven invasion than miR-200a/141 in breast cancer.* Oncogene, 2010. **29**(30): p. 4297-306.
36. Herranz, H. and S.M. Cohen, *MicroRNAs and gene regulatory networks: managing the impact of noise in biological systems.* Genes Dev, 2010. **24**(13): p. 1339-44.
37. Uhlmann, S., et al., *Global microRNA level regulation of EGFR-driven cell-cycle protein network in breast cancer.* Mol Syst Biol, 2012. **8**: p. 570.
38. Tan, X., et al., *miR-638 mediated regulation of BRCA1 affects DNA repair and sensitivity to UV and cisplatin in triple-negative breast cancer.* Breast Cancer Res, 2014. **16**(5): p. 435.
39. Li, Z. and T.M. Rana, *Therapeutic targeting of microRNAs: current status and future challenges.* Nat Rev Drug Discov, 2014. **13**(8): p. 622-38.
40. Janssen, H.L., et al., *Treatment of HCV infection by targeting microRNA.* N Engl J Med, 2013. **368**(18): p. 1685-94.
41. Bouchie, A., *First microRNA mimic enters clinic.* Nat Biotechnol, 2013. **31**(7): p. 577.
42. Agostini, M. and R.A. Knight, *miR-34: from bench to bedside.* Oncotarget, 2014. **5**(4): p. 872-81.
43. Bouwman, P. and J. Jonkers, *The effects of deregulated DNA damage signalling on cancer chemotherapy response and resistance.* Nat Rev Cancer, 2012. **12**(9): p. 587-98.
44. Lohse, I., et al., *BRCA1 and BRCA2 mutations sensitize to chemotherapy in patient-derived pancreatic cancer xenografts.* Br J Cancer, 2015. **113**(3): p. 425-32.
45. Ozols, R.F., *Ovarian cancer: new clinical approaches.* Cancer Treat Rev, 1991. **18 Suppl A**: p. 77-83.
46. Giaccone, G., *Clinical perspectives on platinum resistance.* Drugs, 2000. **59 Suppl 4**: p. 9-17; discussion 37-8.
47. Lebwohl, D. and R. Canetta, *Clinical development of platinum complexes in cancer therapy: an historical perspective and an update.* Eur J Cancer, 1998. **34**(10): p. 1522-34.
48. Rueda, A., et al., *sRNAtoolbox: an integrated collection of small RNA research tools.* Nucleic Acids Res, 2015. **43**(W1): p. W467-73.
49. Lavrik, I.N., A. Golks, and P.H. Krammer, *Caspases: pharmacological manipulation of cell death.* J Clin Invest, 2005. **115**(10): p. 2665-72.

50. Sharma, A., K. Singh, and A. Almasan, *Histone H2AX phosphorylation: a marker for DNA damage.* Methods Mol Biol, 2012. **920**: p. 613-26.
51. Trapnell, C., et al., *Differential gene and transcript expression analysis of RNA-seq experiments with TopHat and Cufflinks.* Nat Protoc, 2012. **7**(3): p. 562-78.
52. Wang, Z., M. Gerstein, and M. Snyder, *RNA-Seq: a revolutionary tool for transcriptomics.* Nat Rev Genet, 2009. **10**(1): p. 57-63.
53. Zhao, S., et al., *Comparison of RNA-Seq and microarray in transcriptome profiling of activated T cells.* PLoS One, 2014. **9**(1): p. e78644.
54. Jiang, L., et al., *MiR-34c oligonucleotide enhances chemosensitivity of Ishikawa cell to cisplatin by inducing apoptosis.* Cell Biol Int, 2013. **37**(6): p. 577-83.
55. Kumaraswamy, E., et al., *BRCA1 regulation of epidermal growth factor receptor (EGFR) expression in human breast cancer cells involves microRNA-146a and is critical for its tumor suppressor function.* Oncogene, 2015. **34**(33): p. 4333-46.
56. Shen, Y., et al., *miR-375 mediated acquired chemo-resistance in cervical cancer by facilitating EMT.* PLoS One, 2014. **9**(10): p. e109299.
57. Bieging, K.T., S.S. Mello, and L.D. Attardi, *Unravelling mechanisms of p53-mediated tumour suppression.* Nat Rev Cancer, 2014. **14**(5): p. 359-70.
58. Damia, G., et al., *Cisplatinum and taxol induce different patterns of p53 phosphorylation.* Neoplasia, 2001. **3**(1): p. 10-6.
59. Zhao, H. and H. Piwnica-Worms, *ATR-mediated checkpoint pathways regulate phosphorylation and activation of human Chk1.* Mol Cell Biol, 2001. **21**(13): p. 4129-39.
60. Appella, E. and C.W. Anderson, *Post-translational modifications and activation of p53 by genotoxic stresses.* Eur J Biochem, 2001. **268**(10): p. 2764-72.
61. Shieh, S.Y., et al., *The human homologs of checkpoint kinases Chk1 and Cds1 (Chk2) phosphorylate p53 at multiple DNA damage-inducible sites.* Genes Dev, 2000. **14**(3): p. 289-300.
62. Delmastro, D.A., et al., *DNA damage inducible-gene expression following platinum treatment in human ovarian carcinoma cell lines.* Cancer Chemother Pharmacol, 1997. **39**(3): p. 245-53.
63. Hershberger, P.A., et al., *Cisplatin potentiates 1,25-dihydroxyvitamin D3-induced apoptosis in association with increased mitogen-activated protein kinase kinase kinase 1 (MEKK-1) expression.* Mol Cancer Ther, 2002. **1**(10): p. 821-9.
64. Smith, M.L., et al., *Interaction of the p53-regulated protein Gadd45 with proliferating cell nuclear antigen.* Science, 1994. **266**(5189): p. 1376-80.
65. Smith, M.L., et al., *The p53-regulated cyclin G gene promotes cell growth: p53 downstream effectors cyclin G and Gadd45 exert different effects on cisplatin chemosensitivity.* Exp Cell Res, 1997. **230**(1): p. 61-8.
66. Alarcon-Vargas, D. and Z. Ronai, *p53-Mdm2--the affair that never ends.* Carcinogenesis, 2002. **23**(4): p. 541-7.
67. Makin, G.W., et al., *Damage-induced Bax N-terminal change, translocation to mitochondria and formation of Bax dimers/complexes occur regardless of cell fate.* EMBO J, 2001. **20**(22): p. 6306-15.
68. Wang, X., J.L. Martindale, and N.J. Holbrook, *Requirement for ERK activation in cisplatin-induced apoptosis.* J Biol Chem, 2000. **275**(50): p. 39435-43.
69. Del Bello, B., et al., *Cleavage of Bcl-2 in oxidant- and cisplatin-induced apoptosis of human melanoma cells.* Oncogene, 2001. **20**(33): p. 4591-5.
70. Micheau, O., et al., *Sensitization of cancer cells treated with cytotoxic drugs to fas-mediated cytotoxicity.* J Natl Cancer Inst, 1997. **89**(11): p. 783-9.
71. Pinto, A.L. and S.J. Lippard, *Binding of the antitumor drug cis-diamminedichloroplatinum(II) (cisplatin) to DNA.* Biochim Biophys Acta, 1985. **780**(3): p. 167-80.
72. Kelland, L.R., *New platinum antitumor complexes.* Crit Rev Oncol Hematol, 1993. **15**(3): p. 191-219.

73. Johnson, S.W., et al., *Increased platinum-DNA damage tolerance is associated with cisplatin resistance and cross-resistance to various chemotherapeutic agents in unrelated human ovarian cancer cell lines.* Cancer Res, 1997. **57**(5): p. 850-6.
74. Yoshida, M., A.R. Khokhar, and Z.H. Siddik, *Cytotoxicity and tolerance to DNA adducts of alicyclic mixed amine platinum(II) homologs in tumor models sensitive and resistant to cisplatin or tetraplatin.* Oncol Rep, 1998. **5**(5): p. 1281-7.
75. Chaney, S.G. and A. Sancar, *DNA repair: enzymatic mechanisms and relevance to drug response.* J Natl Cancer Inst, 1996. **88**(19): p. 1346-60.
76. Larminat, F. and V.A. Bohr, *Role of the human ERCC-1 gene in gene-specific repair of cisplatin-induced DNA damage.* Nucleic Acids Res, 1994. **22**(15): p. 3005-10.
77. Vaisman, A., et al., *The role of hMLH1, hMSH3, and hMSH6 defects in cisplatin and oxaliplatin resistance: correlation with replicative bypass of platinum-DNA adducts.* Cancer Res, 1998. **58**(16): p. 3579-85.
78. Aebi, S., et al., *Loss of DNA mismatch repair in acquired resistance to cisplatin.* Cancer Res, 1996. **56**(13): p. 3087-90.
79. Drummond, J.T., et al., *Cisplatin and adriamycin resistance are associated with MutLalpha and mismatch repair deficiency in an ovarian tumor cell line.* J Biol Chem, 1996. **271**(33): p. 19645-8.
80. Lin, X., et al., *p53 interacts with the DNA mismatch repair system to modulate the cytotoxicity and mutagenicity of hydrogen peroxide.* Mol Pharmacol, 2000. **58**(6): p. 1222-9.
81. Scherer, S.J., et al., *Specific in vitro binding of p53 to the promoter region of the human mismatch repair gene hMSH2.* Biochem Biophys Res Commun, 1996. **221**(3): p. 722-8.
82. Gallagher, W.M., et al., *Identification of p53 genetic suppressor elements which confer resistance to cisplatin.* Oncogene, 1997. **14**(2): p. 185-93.
83. Wattel, E., et al., *p53 mutations are associated with resistance to chemotherapy and short survival in hematologic malignancies.* Blood, 1994. **84**(9): p. 3148-57.
84. Lenz, H.J., et al., *p53 point mutations and thymidylate synthase messenger RNA levels in disseminated colorectal cancer: an analysis of response and survival.* Clin Cancer Res, 1998. **4**(5): p. 1243-50.
85. Marx, D., et al., *Expression of the p53 tumour suppressor gene as a prognostic marker in platinum-treated patients with ovarian cancer.* Eur J Cancer, 1998. **34**(6): p. 845-50.
86. Raza, U., et al., *The miR-644a/CTBP1/p53 axis suppresses drug resistance by simultaneous inhibition of cell survival and epithelial-mesenchymal transition in breast cancer.* Oncotarget, 2016.
87. Siddik, Z.H., *Cisplatin: mode of cytotoxic action and molecular basis of resistance.* Oncogene, 2003. **22**(47): p. 7265-79.
88. Wistuba, II, et al., *Comparison of features of human breast cancer cell lines and their corresponding tumors.* Clin Cancer Res, 1998. **4**(12): p. 2931-8.
89. Takahashi, M., *[Analyses of p53 mutations in breast cancers with a combined use of yeast functional assay and immunohistochemical staining].* Hokkaido Igaku Zasshi, 1998. **73**(3): p. 275-86.
90. Shah, M.A. and G.K. Schwartz, *Cell cycle-mediated drug resistance: an emerging concept in cancer therapy.* Clin Cancer Res, 2001. **7**(8): p. 2168-81.
91. Fan, S., et al., *Cells lacking CIP1/WAF1 genes exhibit preferential sensitivity to cisplatin and nitrogen mustard.* Oncogene, 1997. **14**(18): p. 2127-36.
92. Tsai, C.M., et al., *Enhanced chemoresistance by elevation of p185neu levels in HER-2/neu-transfected human lung cancer cells.* J Natl Cancer Inst, 1995. **87**(9): p. 682-4.
93. Zhou, B.P., et al., *Cytoplasmic localization of p21Cip1/WAF1 by Akt-induced phosphorylation in HER-2/neu-overexpressing cells.* Nat Cell Biol, 2001. **3**(3): p. 245-52.
94. Oliveras-Ferraros, C., et al., *Acquired resistance to metformin in breast cancer cells triggers transcriptome reprogramming toward a degradome-related metastatic stem-like profile.* Cell Cycle, 2014. **13**(7): p. 1132-44.

95. Brady, C.A., et al., *Distinct p53 transcriptional programs dictate acute DNA-damage responses and tumor suppression.* Cell, 2011. **145**(4): p. 571-83.
96. Duan, S., et al., *IL-6 signaling contributes to cisplatin resistance in non-small cell lung cancer via the up-regulation of anti-apoptotic and DNA repair associated molecules.* Oncotarget, 2015. **6**(29): p. 27651-60.
97. Marcelis, C.L., et al., *Genotype-phenotype correlations in MYCN-related Feingold syndrome.* Hum Mutat, 2008. **29**(9): p. 1125-32.
98. Conkrite, K., et al., *miR-17~92 cooperates with RB pathway mutations to promote retinoblastoma.* Genes Dev, 2011. **25**(16): p. 1734-45.
99. Reid, J.F., et al., *miRNA profiling in colorectal cancer highlights miR-1 involvement in MET-dependent proliferation.* Mol Cancer Res, 2012. **10**(4): p. 504-15.
100. Yu, Z., et al., *microRNA 17/20 inhibits cellular invasion and tumor metastasis in breast cancer by heterotypic signaling.* Proc Natl Acad Sci U S A, 2010. **107**(18): p. 8231-6.
101. He, L., et al., *A microRNA polycistron as a potential human oncogene.* Nature, 2005. **435**(7043): p. 828-33.
102. Mogilyansky, E. and I. Rigoutsos, *The miR-17/92 cluster: a comprehensive update on its genomics, genetics, functions and increasingly important and numerous roles in health and disease.* Cell Death Differ, 2013. **20**(12): p. 1603-14.
103. Ventura, A., et al., *Targeted deletion reveals essential and overlapping functions of the miR-17 through 92 family of miRNA clusters.* Cell, 2008. **132**(5): p. 875-86.
104. Houbaviy, H.B., M.F. Murray, and P.A. Sharp, *Embryonic stem cell-specific MicroRNAs.* Dev Cell, 2003. **5**(2): p. 351-8.
105. Farazi, T.A., et al., *MicroRNA sequence and expression analysis in breast tumors by deep sequencing.* Cancer Res, 2011. **71**(13): p. 4443-53.
106. Zhou, P., et al., *miR-17-92 plays an oncogenic role and conveys chemo-resistance to cisplatin in human prostate cancer cells.* Int J Oncol, 2016. **48**(4): p. 1737-48.
107. Agarwal, V., et al., *Predicting effective microRNA target sites in mammalian mRNAs.* Elife, 2015. **4**.
108. Liu, J., et al., *MiR-455-5p acts as a novel tumor suppressor in gastric cancer by down-regulating RAB18.* Gene, 2016.
109. Chai, J., et al., *MicroRNA-455 inhibits proliferation and invasion of colorectal cancer by targeting RAF proto-oncogene serine/threonine-protein kinase.* Tumour Biol, 2015. **36**(2): p. 1313-21.
110. Li, Y.J., et al., *MicroRNA-455 suppresses non-small cell lung cancer through targeting ZEB1.* Cell Biol Int, 2016. **40**(6): p. 621-8.
111. Ujifuku, K., et al., *miR-195, miR-455-3p and miR-10a(*) are implicated in acquired temozolomide resistance in glioblastoma multiforme cells.* Cancer Lett, 2010. **296**(2): p. 241-8.
112. Hummel, R., et al., *Chemotherapy-induced modification of microRNA expression in esophageal cancer.* Oncol Rep, 2011. **26**(4): p. 1011-7.

Appendix

Copyright permission for Figure 1.2 can be found on the next 3 pages.

NATURE PUBLISHING GROUP LICENSE TERMS AND CONDITIONS

Aug 21, 2016

This Agreement between Erol Eyüpoğlu ("You") and Nature Publishing Group ("Nature Publishing Group") consists of your license details and the terms and conditions provided by Nature Publishing Group and Copyright Clearance Center.

License Number	3933630170866
License date	Aug 21, 2016
Licensed Content Publisher	Nature Publishing Group
Licensed Content Publication	Nature Cell Biology
Licensed Content Title	Many roads to maturity: microRNA biogenesis pathways and their regulation
Licensed Content Author	Julia Winter, Stephanie Jung, Sarina Keller, Richard I. Gregory and Sven Diederichs
Licensed Content Date	Mar 1, 2009
Licensed Content Volume Number	11
Licensed Content Issue Number	3
Type of Use	reuse in a dissertation / thesis
Requestor type	academic/educational
Format	print and electronic
Portion	figures/tables/illustrations
Number of figures/tables/illustrations	1
High-res required	no
Figures	Figure 1
Author of this NPG article	no
Your reference number	
Title of your thesis / dissertation	Targeting miRNA-protein regulatory networks to enhance chemotherapy response in BRCA1 mutated TNBCs
Expected completion date	Aug 2016
Estimated size (number of pages)	80
Requestor Location	Erol Eyüpoğlu Bilkent Universitesi 75. Yurt Ankara, 06800 Turkey Attn: Erol Eyüpoğlu
Billing Type	Invoice
Billing Address	Erol Eyüpoğlu Bilkent Universitesi 75. Yurt

Ankara, Turkey 06800
Attn: Erol Eyüpoğlu

Total 0.00 USD

Terms and Conditions

Terms and Conditions for Permissions

Nature Publishing Group hereby grants you a non-exclusive license to reproduce this material for this purpose, and for no other use,subject to the conditions below:

1. NPG warrants that it has, to the best of its knowledge, the rights to license reuse of this material. However, you should ensure that the material you are requesting is original to Nature Publishing Group and does not carry the copyright of another entity (as credited in the published version). If the credit line on any part of the material you have requested indicates that it was reprinted or adapted by NPG with permission from another source, then you should also seek permission from that source to reuse the material.

2. Permission granted free of charge for material in print is also usually granted for any electronic version of that work, provided that the material is incidental to the work as a whole and that the electronic version is essentially equivalent to, or substitutes for, the print version.Where print permission has been granted for a fee, separate permission must be obtained for any additional, electronic re-use (unless, as in the case of a full paper, this has already been accounted for during your initial request in the calculation of a print run).NB: In all cases, web-based use of full-text articles must be authorized separately through the 'Use on a Web Site' option when requesting permission.

3. Permission granted for a first edition does not apply to second and subsequent editions and for editions in other languages (except for signatories to the STM Permissions Guidelines, or where the first edition permission was granted for free).

4. Nature Publishing Group's permission must be acknowledged next to the figure, table or abstract in print. In electronic form, this acknowledgement must be visible at the same time as the figure/table/abstract, and must be hyperlinked to the journal's homepage.

5. The credit line should read:
   Reprinted by permission from Macmillan Publishers Ltd: [JOURNAL NAME] (reference citation), copyright (year of publication)
   For AOP papers, the credit line should read:
   Reprinted by permission from Macmillan Publishers Ltd: [JOURNAL NAME], advance online publication, day month year (doi: 10.1038/sj.[JOURNAL ACRONYM].XXXXX)

   Note: For republication from the *British Journal of Cancer,* the following credit lines apply.
   Reprinted by permission from Macmillan Publishers Ltd on behalf of Cancer Research UK: [JOURNAL NAME] (reference citation), copyright (year of publication)For AOP papers, the credit line should read:
   Reprinted by permission from Macmillan Publishers Ltd on behalf of Cancer Research UK: [JOURNAL NAME], advance online publication, day month year (doi: 10.1038/sj.[JOURNAL ACRONYM].XXXXX)

6. Adaptations of single figures do not require NPG approval. However, the adaptation should be credited as follows:

   Adapted by permission from Macmillan Publishers Ltd: [JOURNAL NAME] (reference citation), copyright (year of publication)

   Note: For adaptation from the *British Journal of Cancer,* the following credit line applies.
   Adapted by permission from Macmillan Publishers Ltd on behalf of Cancer Research UK: [JOURNAL NAME] (reference citation), copyright (year of publication)

7. Translations of 401 words up to a whole article require NPG approval. Please visit http://www.macmillanmedicalcommunications.com for more information.Translations of up to a 400 words do not require NPG approval. The translation should be credited as follows:

   Translated by permission from Macmillan Publishers Ltd: [JOURNAL NAME] (reference citation), copyright (year of publication).

   Note: For translation from the *British Journal of Cancer,* the following credit line applies.
   Translated by permission from Macmillan Publishers Ltd on behalf of Cancer Research UK: [JOURNAL NAME] (reference citation), copyright (year of publication)

We are certain that all parties will benefit from this agreement and wish you the best in the use of this material. Thank you.
Special Terms:
v1.1

Questions? customercare@copyright.com or +1-855-239-3415 (toll free in the US) or +1-978-646-2777.